ResME - A Global Mechanistic Model for Methane Emissions from Hydroelectric Reservoirs

Delwiche, Kyle B.[1]; Harrison, John A.[2], Maasakkers, Joannes D.[3], Sulprizio, Melissa P.[4], Worden, John[5], Jacob, Daniel J.[4], Sunderland, Elsie M.[4]

[1]Department of Earth System Science, Stanford University, Stanford, CA
[2] School of the Environment, Washington State University, Vancouver, WA
[3] SRON Netherlands Institute for Space Research
[4]School of Engineering and Applied Science, Harvard University, Cambridge MA
[5]Jet Propulsion Laboratory, California Institute for Technology, Pasadena, CA, USA

Index terms: Carbon cycling; Biogeochemical cycles, processes, and modeling; Water/energy interactions; Limnology

Keywords: methane, hydropower, reservoirs, degassing, ebullition, diffusion

Key points:

1. Our mechanistic model (ResME) illuminates the main drivers of hydropower methane emissions.
2. Emissions from hydropower turbines are comparable to surface emissions when turbines have deep water intakes.
3. We estimate global emissions from hydropower surfaces as 4.3 Tg C/yr (0.9 – 20.1 Tg C/yr), plus up to 6.6 Tg C/yr from degassing at turbines.

Abstract

Methane (CH_4) emissions from flows through the turbines of hydroelectric reservoirs and newly flooded carbon can contribute to substantially larger CH_4 emissions from reservoirs compared with lakes. As the world economy transitions to renewable forms of energy production, understanding the processes affecting CH_4 emissions from hydroelectric reservoirs is important for developing mitigation efforts. Here we develop ResME ((**Res)**ervoir **(M)e**thane (**E**)missions), the first process-based model of CH_4 emissions that estimates carbon inputs and methanogenesis to mechanistically predict CH_4 release via ebullition and diffusion, plant emissions, and maximum potential turbine emissions. We find that ResME results are correlated with, and relatively unbiased against, field measurements from a subset of global reservoirs ($r^2 = 0.35$, fractional bias = -0.02, n = 57, log-scale), when excluding carbon inputs from allochthonous particulate organic carbon. Mean global estimates of CH_4 diffusive, ebullitive, and plant emissions from all hydroelectric reservoirs in a global database are 4.3 Tg C/yr (0.9 – 20.1 Tg CH_4-C yr^{-1}), with an additional maximum contribution of 6.6 Tg C/yr from turbine emissions at the dams. Turbine emissions have the potential to be globally significant, although the actual contribution will be dependent on turbine intake depths which are unknown for many reservoirs. A preliminary estimate of newly flooded reservoirs suggests that flooded carbon contributes to substantially higher CH_4 emissions over the first 10 years post-flooding compared with after the initial 10-year period, though more field measurements are needed to constrain this contribution.

Plain Language Summary

Methane is an important greenhouse gas and is naturally produced in the sediments of lakes and reservoirs (among many other locations). Hydropower reservoirs produce renewable energy, yet can also emit substantial amounts of methane both from their surfaces and from their turbines and downstream reaches. While some existing studies estimate the global methane release from hydropower, they do not contain the biological, chemical, and physical basis to understand what controls the methane emissions. We have built the Reservoir Methane Emissions model (ResME) using estimations of carbon input, rates of methane production, and

methane movement within the reservoir. ResME results show that excessive algae growth within reservoirs leads to substantially higher methane emissions. We can use the model to understand why certain reservoirs produce more methane than others, and how emissions may change in the future.

1. Introduction

Hydroelectric power is the dominant source of renewable energy globally, comprising 13% of global electricity production in OECD (Organization for Economic Co-operation and Development) countries (International Energy Agency, 2018), and 2.5% of global energy production in 2017. While electricity from hydropower can replace electricity from carbon-intensive sources such as coal and gas, reservoirs also emit methane (CH_4) which could negate some of the carbon benefits of switching to hydropower. CH_4 is a potent greenhouse gas with >32 times the warming potential of carbon dioxide over a 100-year time horizon (Etminan et al., 2016). Multiple international agencies are currently working to quantify and predict CH_4 emissions from hydroelectric facilities. Prior global emissions estimates are 3 Tg C as CH_4 yr^{-1} from reservoir surfaces (Barros et al., 2011), and 13.3 Tg C as CH_4 yr^{-1} from reservoir surfaces, spillways, turbines, river reaches below dams, and periodically inundated drawdown areas around the reservoir (Li & Zhang, 2014). While useful, these estimates were empirical and not based on a mechanistic understanding of reservoir CH_4 production. Here we develop, describe, and apply a new mechanistic model for global CH_4 emissions to the atmosphere from hydroelectric reservoirs. The mechanistic basis of our model provides key insight into the biogeochemical processes controlling hydropower CH_4 emissions, and applying our model globally produces spatially resolved emissions estimates that can be compared with observations.

Hydroelectric reservoirs produce CH_4 via processes similar to those in natural lake ecosystems, with several important differences. In both lakes and reservoirs, carbon inputs come from primary production within the reservoir (Deemer et al., 2016; DelSontro et al., 2019), and inputs of allochthonous carbon from the watershed (Jansson et al., 2007; Jones 1992). In contrast to lakes, hydroelectric reservoirs can also have a large carbon input from the vegetation and soil carbon flooded during reservoir creation, which can fuel CH_4 production. (Abril et al., 2005; Barros et al., 2011; Tremblay et al., 2005; Venkiteswaran et al., 2013). Furthermore,

reservoirs can have enhanced CH_4 production compared to freshwater lakes due to sediment trapping behind dams (Maeck et al., 2013). Methane emissions per square meter are estimated to be roughly 3x higher in reservoirs than in lakes (Deemer et al., 2016). Methane production occurs in sediments where anaerobic microbes respire carbon and produce CH_4. Recent research also suggests that significant quantities of CH_4 are produced within the oxic water column and are associated with primary production (Bižić-Ionescu et al., 2019; Bogard et al., 2014; Grossart et al., 2011; Günthel et al., 2019; Yao et al., 2016).

As with lakes, CH_4 produced in hydroelectric reservoirs can be released via diffusion at the air-water interface, ebullition from the sediments, and vascular transport (Bastviken et al., 2011; Borrel et al., 2011; Casper et al., 2000; Walter et al., 2006). However, in hydroelectric reservoir systems CH_4 can also be emitted at turbine outlets (and immediately downstream of dams), where dissolved CH_4 in the water can quickly degas to the atmosphere (Fearnside 2002; Kemenes et al., 2007). Depending on the CH_4 concentration and the flow rate through the turbines, CH_4 degassing events can be large enough to be seen from space with instruments such as the GHGSat satellite which observed a plume over the Lom Pangar dam in Cameroon (Strupler et al., 2019).

Understanding the global CH_4 emission from hydroelectric facilities is critical to evaluating the carbon-neutrality of this power source. Prior studies have used statistical relationships to predict atmospheric CH_4 emissions from reservoir properties such as littoral area, mean annual temperature, age, chlorophyll *a* concentration, and mean depth (Barros et al., 2011; Deemer et al., 2016; DelSontro et al., 2019). Predictor variables such as total phosphorus, latitude, and temperature are inconsistent across studies, and some models neglect emissions from turbine degassing and downstream emissions, which can be comparable to emissions from ebullition (Deemer et al., 2016). More recently, the GHG Reservoir Tool (G-RES) has been developed to help reservoir managers estimate potential CH_4 emissions (Prairie et al., 2017). While the G-RES tool includes the most thorough consideration of reservoir greenhouse gas emissions to date, including estimations of emissions prior to reservoir construction and during dam building, it still relies on empirical relationships to estimate CH_4 emissions from multiple environmental drivers. The main objective of this work is to formalize our understanding of the physical drivers of CH_4 emissions from hydroelectric reservoirs in a global, mechanistic model

for CH_4 emissions to the atmosphere ((Res)ervoir (M)ethane (E)missions model, or ResME). While existing estimates of CH_4 emissions from reservoirs and hydropower facilities rely on empirical associations with environmental parameters, our model is based on fundamental biogeochemical modeling with no empirical fitting.

We evaluate the model using available measurements of CH_4 emissions from 57 hydroelectric facilities. We apply the model to estimate the potential contribution of turbine outflow CH_4 emissions to total reservoir emissions, as well as the potential contribution from the biomass flooded during reservoir creation. We construct a global, spatially resolved inventory of CH_4 emissions from hydroelectricity that can be used as prior estimate in inversions of atmospheric CH_4 observations. We use our analysis to identify key uncertainties in processes affecting global CH_4 from hydropower facilities and discuss data needed to improve future emissions projections.

2. Model Development

ResME includes parameterizations for (Figure 1):

(1) Carbon inputs to methanogenesis from flooded soil and biomass carbon, autochthonous input, and allochthonous input
(2) CH_4 production in anoxic sediment
(3) CH_4 release via diffusion, ebullition, and vascular transport, and turbine degassing release (which depends on turbine intake depth).

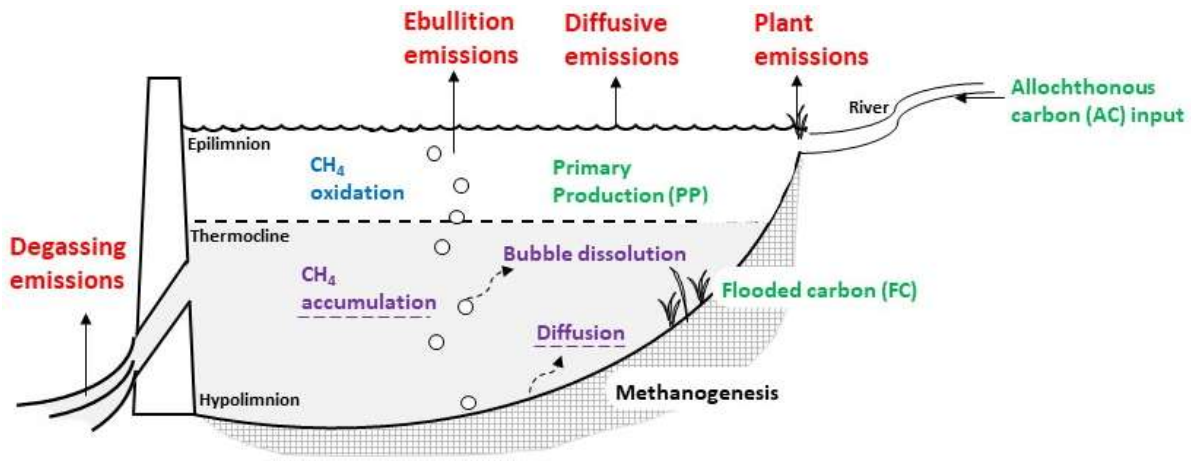

Figure 1. Schematic of hydroelectric reservoir and factors contributing to CH_4 production and transport. Carbon sources for methanogenesis are shown in green, CH_4 emissions pathways in red, CH_4 removal pathway in blue, and internal CH_4 fate/transport pathways in purple. Dashed arrows indicate internal transport. All sources and fates shown are explicitly modeled, except for those with dashed underlines (diffusion and CH_4 accumulation).

2.1 Carbon inputs to methanogenesis from autochthonous input, allochthonous input, and flooded carbon

We include three sources of organic carbon (C_t in Equation 1) as substrate for methanogenesis: a) autochthonous carbon generated by primary producers (such as algae) within the reservoir; b) allochthonous carbon from connecting rivers; and c) the soil carbon and biomass carbon present in the reservoir landscape prior to flooding.

2.1.1 Autochthonous input

We estimate autochthonous carbon (carbon coming from inside the aquatic system, in this case the reservoir) primary production in different reservoirs using literature-reported trophic status. Trophic status is a categorization reflecting the amount of biological productivity occurring in a water body. Trophic status is reported in the literature as oligotrophic (low productivity), mesotrophic (medium productivity), or eutrophic (high productivity). Each trophic state has a characteristic range of nutrient loading, chlorophyll *a* concentration, and

158 primary productivity (such as algal growth) (Wetzel, 2001). Primary production in freshwater
159 systems ranges from less than 50 mg C m^{-2} day^{-1} for oligotrophic systems to ~8000 mg C m^{-2}
160 day^{-1} for some highly eutrophic systems (Likens, 1975; Wetzel, 2001). Based on numerous field
161 measurements, we estimate mean primary production for oligotrophic, mesotrophic, and
162 eutrophic reservoirs as 151, 570, and 2019 mg C m^{-2} day^{-1}, respectively (Kimmel *et al*. 1990).

163 Not all autochthonous carbon settles to the sediment where it is available for
164 methanogenesis. The amount of autochthonous carbon that settles has been estimated as around
165 80% by Teodoru et al., 2013, and 20% by Ostrovsky and Yacobi, 2010; we use an intermediate
166 value of 50%.

167 2.1.2 Allochthonous input

168 Allochthonous carbon is carbon sourced from outside the aquatic system, such as from
169 the surrounding watershed. Dissolved and suspended particulate organic carbon (DOC and POC,
170 respectively) is delivered to reservoirs by rivers, and a portion of each carbon form is
171 subsequently buried in the sediment (Wachenfeldt et al., 2009). We estimate POC inputs to
172 sediment based on the total river sediment load (Equation S1-S2; Meybeck, 1982). Total
173 sediment load is predicted from drainage basin size, relief, temperature, soil freeze/thaw cycles,
174 and soil formation rates (Syvitski et al., 2003). Allochthonous POC input is then estimated as a
175 function of total sediment load (Beusen *et al,* 2005). Since not all sediment entering the
176 reservoir will be trapped, we estimate trapping efficiency based on hydraulic residence time
177 (Equation S3, Vorosmarty et al., 2003). The ratio of DOC to total organic carbon (DOC + POC)
178 has been found to decrease with increased suspended sediment load (Equation S4; Meybeck,
179 1982). Flocculation (fine particles clumping together and settling) rates for incoming DOC vary
180 with temperature (Equation S5, Wachenfeldt et al., 2009). Additional details are available in the
181 Supporting Information, including Tables S1-S3.

182 2.1.3 Flooded carbon

183 Annual average organic carbon for 12 different carbon pools (including leaf, fine root,
184 wood, and woody debris pools, as well as metabolic, structural, and microbial pools both above
185 and below ground) within each flooded reservoir is estimated based on a global terrestrial carbon

model with 0.5 x 0.5 degree gridded monthly resolution (SibCASA, Schaefer et al., 2008). Flooded carbon input at the time of reservoir creation was assumed to be the sum of the SibCASA carbon pools at the reservoir location. Since lignin inhibits decay (Van Coillie et al., 1983) to the point that no wood decay was observed in a recently flooded reservoir (Hall and St Louis, 2004), we excluded the SibCASA carbon pools of wood and woody debris.

2.2 Methane production in anoxic sediment

We model daily CH_4 production (P_t, mg CH_4 m^{-2} day^{-1}) associated with decay of organic carbon following (Vachon et al., 2017):

$$P_t = \frac{dC}{dt} = 0.5 \times \underline{k_t} \times C_t \quad (1)$$

where C_t is the bulk carbon content of age t in the sediment (mg C m^{-2}), $\underline{k_t}$ is the age-dependent decay constant for the mixture of organic material, and 0.5 reflects the fact that some carbon is converted to CO_2 instead of CH_4 (the exact ratio depends on the fraction of aerobic to anaerobic decomposition and the ratio of acetoclastic to hydrogenotrophic methanogenesis (Conrad et al., 2005), which is beyond the scope of ResME to determine). Since Equation 1 represents the methanogenesis for carbon of a particular age, carbon pools containing carbon of different ages will require a sum of P_t values (see Equation 3).

2.2.1 Reactive continuum model for organic carbon decay (k)

Recent work has shown that reactive continuum decay models successfully predict decay patterns for heterogeneous carbon pools (Catalan et al., 2017; Koehler et al., 2015). Reactive continuum models allow the decay rate (k_t-) to vary based on organic carbon type, and to change during the decomposition process as labile compounds are consumed (Boudreau and Ruddick, 1991; Koehler et al., 2012; Mostovaya et al., 2017; Vachon et al., 2017). Variable decay rates are important because biomass from autochthonous primary production is more readily degraded by methanogens compared to other terrestrial carbon sources (Gudasz et al., 2012; West et al.,

2016; Zhou et al., 2019). Additionally, non-lignin components of biomass are more labile than wood, which is relatively recalcitrant (Moran et al., 1989; Koehler and Tranvik, 2015).

We used the reactive continuum decay model to estimate the apparent decay constant, k, following the parameterization described by (Boudreau et al., 2008), and the Arrhenius correction for temperature described by (Venkiteswaran et al., 2007):

$$\underline{k} = \frac{v}{(a+t)} \times 1.047^{(T-20)} \quad (2)$$

where t is carbon age (in days), α is a rate parameter related to the average lifetime of the more labile carbon compounds, v is a unitless parameter related to the relative abundance of more recalcitrant compounds (Boudreau et al., 2008), and T is sediment temperature (C). The parameters α and v have been determined experimentally by others for a range of organic matter types, and the parameter values (with literature sources) we use in ResME are provided in Table 1 (discussed below). Values for riverine carbon are taken from Vachon et al. (2017). Autochthonous decay parameters were estimated from decay experiments using DOC from clearwater lakes, which are higher in autochthonous carbon than dystrophic lakes (Koehler et al., 2012). For flooded carbon, we use average values of α and v from a leaf litter decomposition study by Koehler and Tranvik (2015). Since Koehler and Tranvik (2015) studied leaf decomposition in air, we multiplied α, the average lifetime of the more labile carbon compounds, by 0.5 based on experiments showing underwater decay is roughly twice as fast as decay in air (Hall and St. Louis, 2004).

Table 1: Decay constants used in reactive continuum decay modeling for autochthonous, allochthonous, and flooded carbon sources.

	α^1 *(days)*	v^2 *(dimensionless)*
Autocthonous carbon	25.2[3]	0.11[3]
Allocthonous carbon	55.3[4]	0.137[4]
Flooded carbon	354[5]	0.84[5]

Note:

[1] Average lifetime of the more reactive compounds

[2] Relative abundance of the most recalcitrant compounds

[3] Koehler et al., 2012. Values measured for primarily autochthonous DOC.

[4] Vachon et al., 2016. Average values measured for allochthonous DOC.

[5] Koehler et al., 2015. Average values measured for leaf decomposition. Since decomposition was measured in air, and plant matter decomposition is faster underwater (Hall and St. Louis, 2004), α values were decreased by half.

Allocthonous and autochthonous carbon are continually being added to a reservoir system, which requires additional terms to Equation 2. Upon addition to the model reservoir, a portion of this 0-day-old carbon is mineralized (following Eqs. 1 and 2, where $t = 0$) and the remainder rolls over into the 1-day-old carbon pool where t becomes 1 (Figure 2). The modeling therefore requires accounting for the daily input of fresh carbon, the transfer of unmineralized carbon after each day to the next oldest age pool, and different decay parameters for every age pool. After accounting for these additions, the total CH_4 production (P_{tot}) for a reservoir of age A is:

$$Ptot = \sum_{Csource} \sum_{t=0}^{A} \frac{v}{\alpha+t} \times C_t \times 1.047^{(T-20)} \quad (3)$$

Where t is the age of the carbon input in each daily age class, A is the current age of the reservoir, T is the sediment temperature, C_t is the carbon content in each daily age class, and

results from different carbon sources (C_{source}) are summed. Running a decay model with a daily timestep is computationally expensive. To simplify the process, we created a series of look-up tables for a range of reservoir ages and temperatures (Tables S4-S6). Methane production is estimated by multiplying the values in the look-up table by the daily carbon input value (ie: daily autochthonous or allochthonous loading in g/m^2). We created three different tables for the combinations of α and v for flooded carbon, allochthonous input, and autochthonous input (α and v from Table 1*)*. The maximum reservoir age in the look-up tables is 100 years, since values for autochthonous and allochthonous carbon-based production were found to change less than 0.1% per year after 100 years, and flooded carbon-based CH_4 production is negligible after 100 years). For reservoirs older than 100 years, we use the look-up parameter for 100-year-old reservoirs in Tables S4-S6. By using the look-up tables, total CH_4 production (P_{tot}) is simplified to:

$$P_{tot} = R_1(A,T) \times AutoC + R_2(A,T) \times AllocC + R_3(A,T) \times FloodedC \quad (4)$$

Where *AutoC* and *AllocC* are the daily inputs of autochthonous and allochthonous carbon, respectively, and *FloodedC* is the biomass and soil carbon flooded during reservoir creation (in mg CH_4-C/m^2). R_1, R_2, R_3 are the look-up parameters from Tables S4-S6 for autochthonous carbon, allocthonous carbon, and flooded carbon (respectively) for each reservoir's age (A) and sediment temperature (T) (sediment temperature calculations described below).

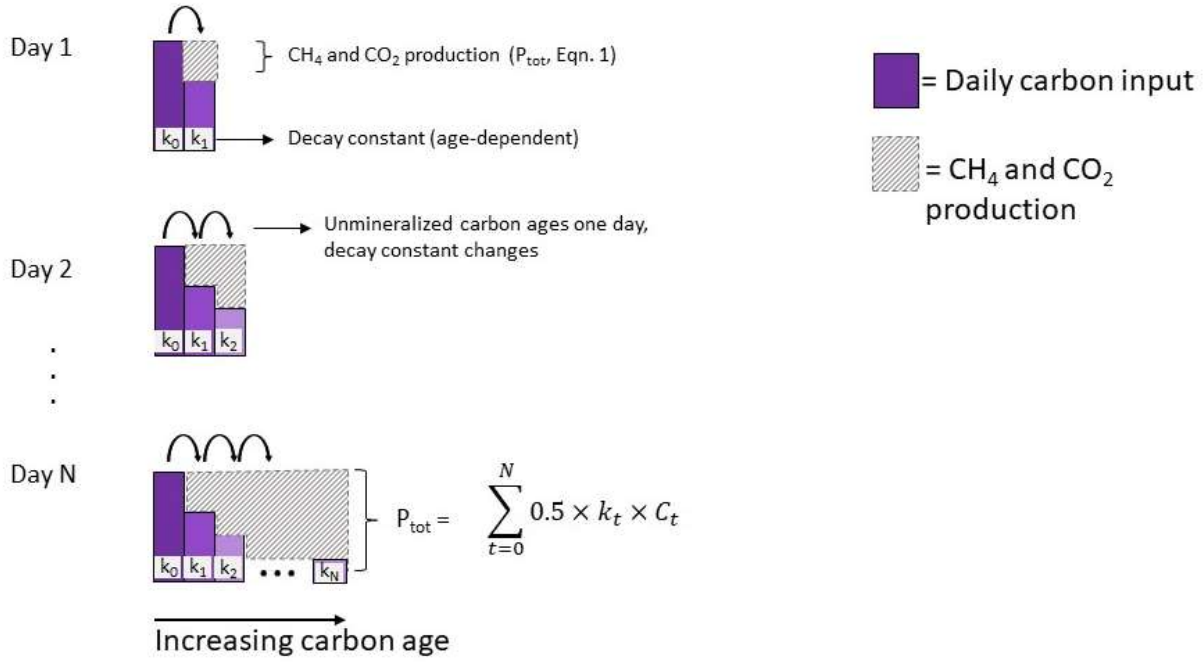

Figure 2: Model schematic showing carbon pool progression across lifetime of reservoir (age = *N*), for one carbon type. Total methanogenesis (P_{tot}) is the sum of methanogenesis from each carbon type (autochthonous, allochthonous, and flooded carbon). Variable descriptions are associated with Equations 1 and 2 in the main text.

2.2.2 Sediment temperature

Sediment temperature affects methanogenesis rates, and is therefore necessary to calculate total CH_4 production. Sediment temperature is tied to reservoir stratification status, with sediments in deeper, unmixed waters being colder than littoral, well mixed waters. Sediment temperature in the hypolimnion can be estimated as a function of latitude (Equation S7), and peak epilimnetic temperatures can be modelled based on mean July air temperature (January for the Southern Hemisphere), mean annual air temperature, Julian date of maximum temperature, and longitude (Equation S6) (Sharma et al., 2007). The occurrence and duration of stratification is a function of parameters such as water transparency, wind speed, and reservoir morphology, and can be modeled with significant input data (Lee et al., 2013; Noori et al., 2019; Yigzaw et al., 2019). For simplicity, and to allow for ResME application in systems without detailed information, we assume that sediment temperature under water columns less than 5 m deep equals peak epilimnetic temperature (Equation S6) for 2 months per year. Temperatures the

remainder of the year, and for all depths greater than 5 m, are equal to the hypolimnetic temperature (Equation S7). We assess the model sensitivity to temperature assumptions in the Sensitivity Analysis section.

To translate the epilimnetic temperatures and hypolimnetic temperatures to an areal basis, we needed to estimate the fraction of each reservoir with sediments above and below 5 m. While we do not have detailed bathymetry for each reservoir in the set of reservoirs with field CH_4 estimates that we use for model comparison, the Global Reservoir and Dam Database (GRanD) database provides footprints for many reservoirs (Lehner et al., 2011). We can simulate the bathymetry of each reservoir by assuming a linear slope between reservoir shore and the maximum basin depth at the maximum distance from shore (Figure 3). The resulting sediment slope provides an estimated water column depth throughout the reservoir (see Figure 3 inset). For all reservoirs, dam heights are available from GRanD or individual sources (see Table S7). We estimate the maximum reservoir depth as 90% of the dam height, thereby roughly accounting for the vertical distance between the designed water surface and the top of the channel bank (freeboard). We use this modeled bathymetry to estimate the sediment surface area at depths greater and less than 5m. For reservoirs in our comparison data set that do not have GIS footprints in GRanD, we assume the ratio of epilimnetic to hypolimnetic sediments is 0.5.

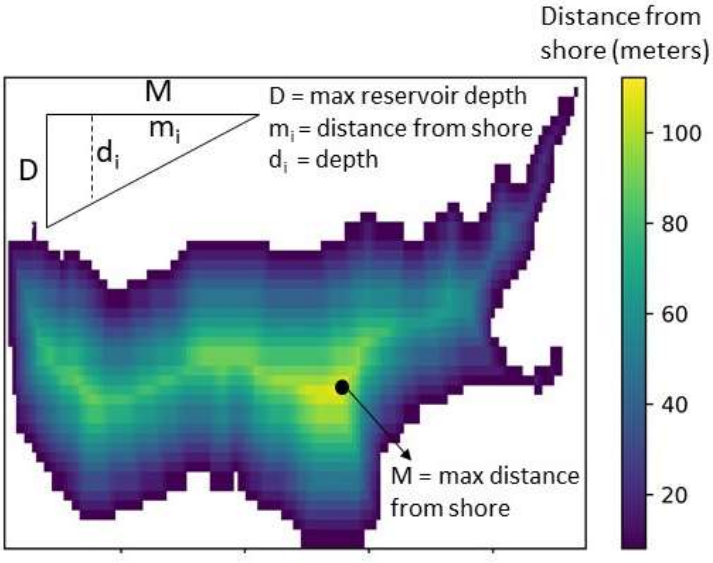

Figure 3: Estimated bathymetry for Foster reservoir in Oregon, USA based on the reservoir footprint and maximum depth.

2.3 Methane release via diffusion, ebullition, and vascular transport, and turbine degassing release assuming deep water turbine intake.

The fate of CH_4 produced in the reservoir sediment (P_{tot}, mg C/m^2/day, Equation 5) is partitioned by mass balance in to five potential fates:

$$P = Ox + E_b + D_f + T_b + A_p \quad (5)$$

where Ox is internal oxidation, E_b is ebullition, D_f is diffusive emission, T_b is emission through turbines (or immediately downstream of the dam), and A_p is transport through plant tissue (parameter estimates explained below). The balance of CH_4 partitioning between oxidation, diffusion, ebullition, turbine output, and plant tissue is determined by complex interactions between physical, chemical, and biological forces across both space and time. ResME uses simple theoretical relationships and literature estimates to parameterize and estimate the five potential CH_4 fates.

2.3.1 Oxidation and Turbine Emissions

Internal oxidation within a stratified reservoir is thought to occur primarily along the oxycline, where CH_4 diffuses upwards and encounters methanotrophs in aerobic water. Methane is rapidly depleted at the oxycline, and the amount of CH_4 diffusing upwards determines the rate of oxidation. Processes that decrease the amount of dissolved CH_4 in the hypolimnion of the reservoir will decrease internal CH_4 oxidation at the oxycline. Thus, turbines that pull water from a CH_4-rich hypolimnion will directly reduce the amount of CH_4 available for oxidation. Turbines that pull water from a CH_4-poor epilimnion should not affect oxidation rates. ResME therefore assumes Ox and T_b are directly and negatively coupled such that increased CH_4 release through the turbines leads to a decrease in internal oxidation within reservoirs. ResME does not include emissions estimates for the fall, when potentially CH_4-rich water from the hypolimnion gets mixed with the epilimnion ("fall turnover") and can therefore diffuse to the atmosphere.

Some studies suggest that CH_4 oxidation during fall turnover is rapid enough to prevent significant fall CH_4 emissions (Utsumi et al., 1998; Kankaala et al., 2007; Schubert et al., 2012.; Mayr et al., 2020), though this is not true for all water bodies (Fernandez et al., 2014).

Much of the literature on whole-system oxidation rates (*Ox*) comes from relatively shallow lakes, where oxidation is found to consume roughly 50% of total CH_4 production. (Almeida et al., 2016; Bastviken et al., 2008; Schmid et al., 2017). This estimate for oxidation as a percentage of production in shallow lakes can be expanded to deeper water bodies by considering that in deep water, bubble dissolution can contribute significantly to the amount of dissolved CH_4 available for oxidation (Delwiche and Hemond, 2017; Schmid et al., 2017). The amount of bubble dissolution is a function of reservoir depth (McGinnis et al., 2006). We therefore assume that total potential oxidation (*Ox*) is a minimum of 50% of total CH_4 production, plus a depth-dependent fraction to account for bubble dissolution:

$$Ox + T_b = (0.5 + Bub_{diss}) \times P \qquad (6)$$

where Bub_{diss} describes a linear increase in oxidation and/or turbine release with reservoir depth (described below). Thus, we estimate that when turbines pull from the hypolimnion, maximum potential turbine release is (0.5 + Bub_{diss}) x *P*, and internal oxidation is zero. Conversely, turbine release is assumed to be zero when turbines pull from the epilimnion, and internal oxidation is (0.5 + Bub_{diss}) × *P*.

To estimate Bub_{diss}, we first recognize that bubbles in aquatic systems are typically around 5mm in diameter (DelSontro et al., 2015; Delwiche and Hemond, 2017; Ostrovsky et al., 2008), and 5 mm bubbles are expected to completely dissolve in 60m water columns (McGinnis et al., 2006). We therefore model the spatially average Bub_{diss} as:

$$Bub_{diss} = \begin{cases} 0.3 \times \frac{d}{60} & for\ d < 60m \\ 0.3 & for\ d \geq 60m \end{cases} \qquad (7)$$

where *d* is the average reservoir depth (m). The 0.3 parameter represents the maximum fraction of CH_4 production that could contribute to bubble dissolution. This parameter is less

than 0.5 because even in deep systems, some of the produced CH_4 will still escape to the atmosphere from littoral zones.

2.3.2 Plant emissions

Total transport through vascular plant tissue (A_p) depends on many factors, including plant type, water column depth, plant coverage, and length of vegetation period. Bastviken et al. (2011) estimate vascular plant transport (A_p) at approximately 16% of emissions due to diffusion and ebullition ($E_b + D_f$):

$$A_p = 0.16 \times (E_b + D_f) \quad (8)$$

2.3.3 Diffusive and ebullitive emissions

Combining Equations 5-8 yields an estimate of ebullitive and diffusive emissions that depends on total CH_4 production (P_{tot}) and the depth-dependent parameter Bub_{diss}:

$$E_b + D_f = \frac{P}{1.16}[1 - 0.5 \times Bub_{diss}] \quad (9)$$

Many field studies report ebullition and diffusion estimates from reservoir surfaces, and we can compare these field estimates with the estimations from Equation 9.

3.0 Evaluating Model Methodology

We ran ResME for a subset of global reservoirs with the necessary ancillary information to estimate all model parameters. In addition to comparing CH_4 emissions from ResME to field

data, we also assessed ResME calculations for the key parameters of sediment temperature and allochthonous carbon inputs. We focused on allochthonous carbon inputs because these were calculated based on watershed parameters and were not constrained by measurements, whereas autochthonous carbon and flooded carbon were already based on published assessments of trophic status (for autochtonous carbon), or published global carbon maps (flooded carbon).

3.1 Field measurements for comparison

We found 57 hydroelectric reservoirs (hereafter referred to as the "reservoir subset") with corresponding diffusive and ebullitive CH_4 measurements, and all necessary ancillary information for ResME. Many of these studies were compiled by Barros et al., 2011, Deemer et al., 2016, and Prairie et al., 2017, with a few more having been published more recently (Table S7). These reservoirs represent a range of sizes, flow rates, and geographical locations spanning the globe (Figure 4). We can compare these reservoirs to the 2,462 hydropower reservoirs in GRanD, where GRanD is a global, geographically referenced list of reservoirs and associated metadata (Lehner et al., 2011). The reservoir subset over-represents large reservoirs compared to their size-based prevalence in GRanD, while flow rates and latitude are more representative of GRanD values (Figure S1). The 57 reservoirs in our subset represent 12% of the discharge from all reservoirs in the GRanD database, which reflects the fact that our reservoir subset is skewed towards large systems. Reservoirs in the subset contain a relatively even mix of trophic statuses (21 oligotrophic to oligo-mesotrophic reservoirs, 17 mesotrophic reservoirs, and 20 meso-eutrophic to eutrophic reservoirs).

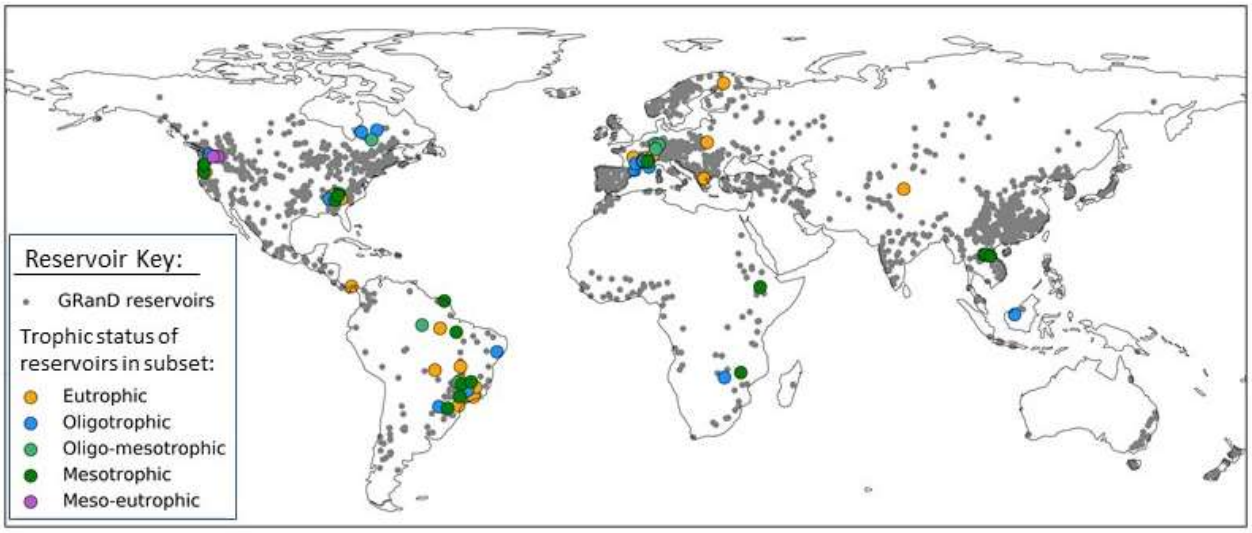

406

407 **Figure 4:** All hydroelectric reservoirs in the GRanD database (grey dots). Reservoirs with field
408 data that were compared to model results ("reservoir subset") are colored based on trophic status.
409

410 ## 3.2 Temperature results

411 We compared model outputs (see Table S8) to field measurements for hypolimnetic and
412 epilimnetic temperature from the reservoir subset. ResME maximum surface water temperatures
413 approximately match measured peak water temperatures across a wide range of latitudes (Figure
414 S2a). Modeled hypolimnetic temperatures were systematically lower than measured values by 6
415 +- 2 °C (Figure S2b), which may be because Equation S7 for hypolimnetic temperature was
416 derived for lakes, whereas reservoirs have different hydrodynamics. To assess the impact of a
417 bias in hypolimnetic temperatures, we increased hypolimnetic temperatures by 5% in our model
418 sensitivity analysis (discussed below).
419

420 ## 3.3 Allochthonous carbon inputs

421 To assess the representativeness of the allochthonous POC inputs calculated in ResME,
422 we compared ResME estimates of riverine total suspended solids (TSS) and POC concentration
423 to global compilations of river measurements from the GEMS-GLORI database (Meybeck and

Ragu, 2012) (Figure S3). The ResME distribution of TSS concentrations in our reservoir subset is significantly higher than the global distribution in GEMS-GLORI ($p < 0.001$, using a Kolmogorov-Smirnov test). Global mean and median TSS values are 1918 and 194 mg/L, respectively, while mean and median TSS from the ResME reservoir subset are 2295 and 677 mg/L, respectively. Similarly, estimates for riverine POC are also higher than the global distribution from GEMS-GLORI ($p < 0.001$), with mean[median] of 8.9[2] mg/L globally, and 27[5.8] mg/L for the reservoir subset (Figure S4). This could either be because ResME overestimates riverine POC inputs, or because our reservoir test set is systematically biased towards rivers with higher POC concentrations. We discuss this further below.

4.0 Evaluating Model Results

4.1 Contribution of each carbon source to methanogenesis

For most of the reservoir subset, ResME estimates that the majority of methanogenesis comes from the decay of autochthonous carbon and allochthonous POC inputs (26 ± 25% and 62 ± 29% of total methanogenesis, respectively), with the remaining coming from allochthonous DOC and flooded carbon inputs (5 ± 5% and 7 ± 19% of total methanogenesis, respectively) (Figure 5). Allochthonous POC tends to be more important for oligotrophic and mesotrophic systems, whereas autochthonous carbon is the primary carbon source for methanogenesis in many of the eutrophic reservoirs. Allochthonous inputs from flocculated DOC comprises at most 29% of methanogenesis, and flooded carbon only exceeds 10% of total methanogenesis in 5 of the 57 reservoirs (average age of 5 reservoirs with highest methanogenesis from flooded biomass = 5 years). The relative contribution of flooded biomass to total methanogenesis is highly dependent on reservoir age. Since the average age of reservoirs within our subset is 50 years, the CH_4 contribution from flooded biomass is relatively low. Relative contributions from flooded carbon dominate in very young systems (Figure 5).

While the relative contributions from different carbon sources are useful for understanding the dominant drivers of methanogenesis in reservoirs, the uncertainty associated

with these estimations is high. For example, while we have chosen single values of primary production for each trophic status, the ranges of potential primary production within each trophic status vary widely (Wetzel, 2001). The relative simplicity of ResME calculations allows the model to be applied to a global range of reservoirs even with minimal site-specific information. However, reducing uncertainty in reservoir-specific modeling results would require more detailed site-level input information and modeling parameters.

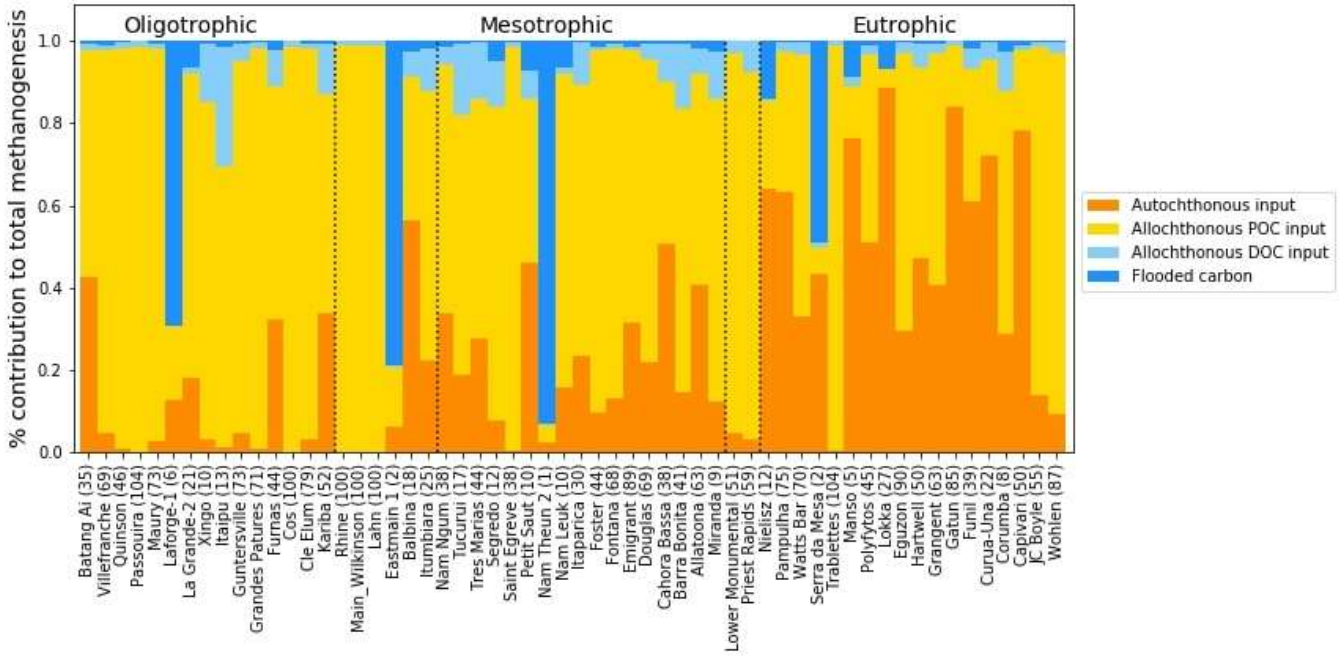

Figure 5. Carbon source for daily methane (CH_4) production, shown as percentage of total methanogenesis, and colored by carbon type. Reservoirs are grouped by trophic status, and parenthetical numbers after reservoir names are reservoir ages, in years.

4.2 Ebullitive and diffusive emissions, with contributions from each carbon source

ResME predictions for ebullitive and diffusive CH_4 emissions are correlated with, but substantially over-predict, field measurements ($r^2 = 0.23$, $p = 0.0001$, mean fractional bias = 0.86). Here we use the mean fractional bias (MFB) to estimate how biased ResME estimates are compared with field observations of CH_4 flux. MFB is:

$$MFB = \frac{2}{N}\sum_{i=1}^{N} \frac{C_{m,i} - C_{o,i}}{C_{m,i} + C_{o,i}}$$

where C_m and C_o are the model-predicted and observed ebullition plus diffusion flux (respectively), and N is the number of reservoirs (Boylan et al., 2006, Zhang et al., 2014). Sequentially removing carbon inputs from the model allows us to assess the relative importance of each carbon source to model fit (Figure 6). Removing allochthonous POC loading from the model substantially improves model fit ($r^2 = 0.35$) and prediction bias (MFB = -0.02). Removing the flooded carbon inputs have minimal effect on model fit to field data (likely because average reservoir age is 47 years and flooded carbon is mostly decayed at this point), but increases the average amount by which ResME underestimates CH_4 flux ($r^2 = 0.34$, MFB = -0.19, Figure 6c). Autochthonous carbon alone, which has been found in previous studies to be a suitable proxy for CH_4 emissions (estimated by chlorophyll a concentration: Deemer *et al*., 2016; DelSontro *et al*., 2019), generates reasonable fits between measurements and model for reservoirs with longer water residence time (Figure 6d). However, run-of-river reservoirs with small water residence times, are not well described with only autochthonous carbon. This could indicate that allochthonous carbon plays a larger role in reservoir CH_4 emissions for reservoirs with short residence times, compared to reservoirs with long residence times.

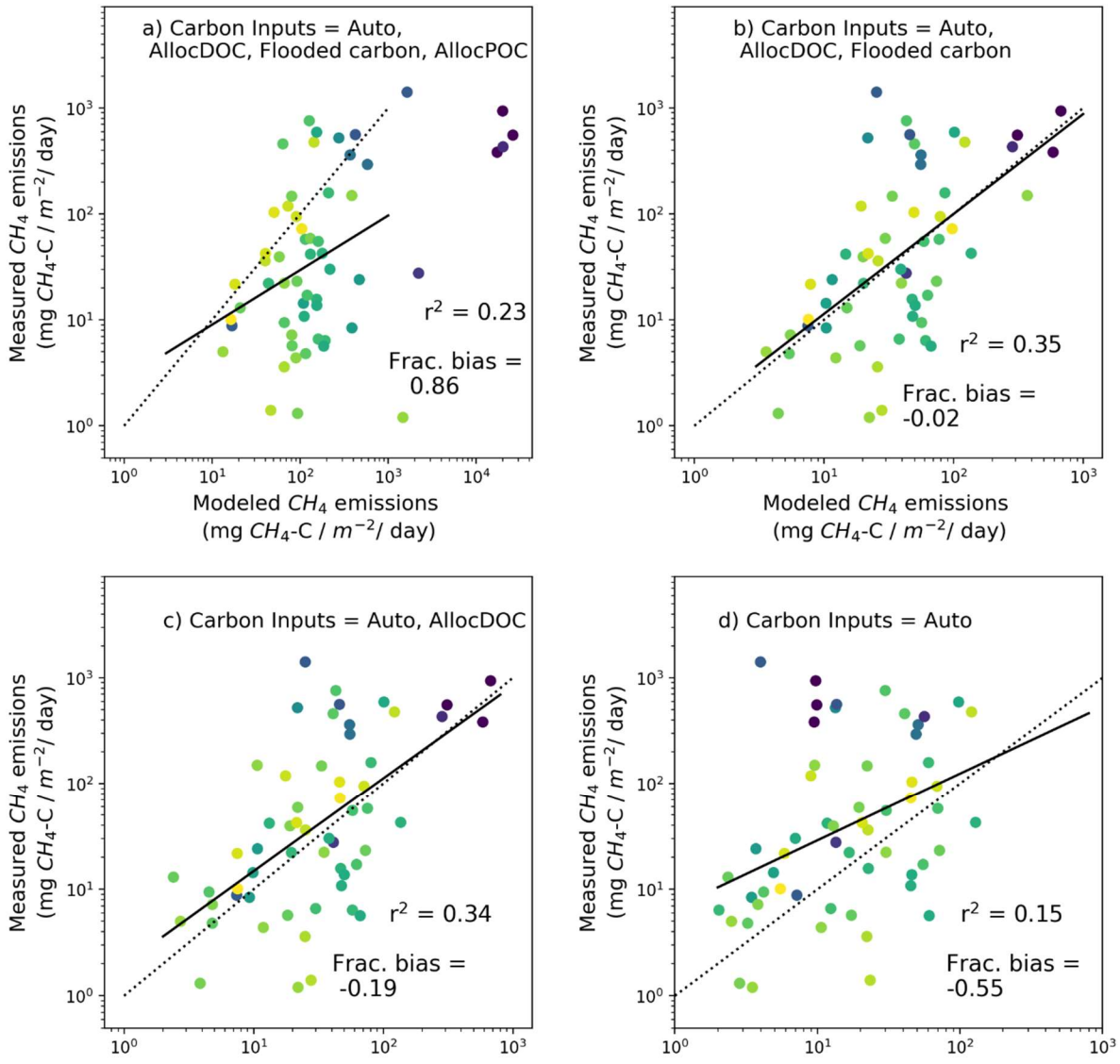

Figure 6: Comparing field measurements of methane (CH_4) flux to model output, where carbon source for methanogenesis includes autochthonous carbon, allochthonous DOC and POC, and flooded carbon (a), autochthonous carbon, allochthonous DOC, and flooded carbon, (b), autochthonous carbon and allochthonous DOC (c), and autochthonous carbon (d). Solid black lines are regression fits, and dotted black lines represent a 1:1 relationship between measured and modeled CH_4 emissions. Marker colors indicate reservoir residence time, where darker colors are shorter times.

497 The improved fit when eliminating allochthonous POC input could indicate that ResME
498 over-predicts methanogenesis from allochthonous POC, or that field measurements of CH_4
499 release do not adequately capture CH_4 emissions due to allochthonous POC inputs. For ResME
500 to over-predict CH_4 production due to allochthonous POC, either the input estimates of POC
501 would need to be erroneously high, or the material would need to be more recalcitrant than our
502 decay constants predict. We did find that the distribution of ResME-estimated allochthonous
503 POC inputs is substantially higher than the global distribution, with mean values from ResME
504 being an order of magnitude higher than global data (Figure S4). While this mismatch could be
505 because our reservoir subset is not representative of global reservoirs, the very large difference
506 suggests at least some over-estimate of allochthonous POC contributions to hydropower
507 reservoirs.
508
509 Field measurements could potentially underestimate CH_4 emissions due to allochthonous
510 POC inputs because these inputs are typically non-homogeneous in space. Allochthonous POC
511 tends to settle out in reservoir inflow deltas, and this spatially heterogeneous loading of
512 allochthonous input has been found to create substantially higher CH_4 emission rates in upstream
513 areas of reservoirs (Beaulieu et al., 2014; DelSontro et al., 2011; Grinham et al., 2011; Musenze
514 et al., 2014). Indeed, Grinham et al. (2011) found that up to 97% of CH_4 release comes from 1.8-
515 7% of total surface area, primarily concentrated at the upstream boundaries of the reservoir.
516 Since not all studies of overall reservoir CH_4 emissions sample specifically from the river mouth,
517 these elevated emissions driven by allochthonous POC input may not be reflected in reported
518 reservoir emission rates. Given the large uncertainty with the role of allochthonous POC
519 estimates, going forward we present results both with and without this carbon input.

520 4.3 Turbine emissions

521 Methane emission estimates for maximum potential turbine degassing can be compared
522 to field campaigns measuring degassing at reservoirs where turbine water intake is well below a
523 stratified thermocline (the theoretical maximum degassing calculated by ResME occurs from
524 deep turbine intakes). We found 4 previously studied reservoirs with annual degassing estimates
525 from deep-water intakes, and the ResME maximum theoretical turbine degassing is 54 ± 34% of
526 the measured degassing (when excluding allochthonous POC inputs; when including

allochthonous POC, measured degassing is 111± 70% of measurements (Table 2)). ResME estimates are even lower than field estimates when we consider that some of the dissolved CH_4 that passes through turbines will be oxidized instead of released to the atmosphere. For example, approximately 10% of the CH_4 released through turbines at the Petit-Saut dam is internally oxidized (Fearnside, 2002), whereas approximately 40% of CH_4 released through turbines in Balbina is oxidized (Kemenes et al., 2007). While ResME provides a reasonable order-of-magnitude estimate of CH_4 turbine degassing at turbine outlets, accurately upscaling estimates of turbine CH_4 outputs would require information about turbine intake height at each reservoir. Field measurements for systems that pull water from the epilimnion are dramatically lower than those systems which draw water from the hypolimnion, since the epilimnion waters are much lower in dissolved CH_4 (Chanudet et al., 2011).

Table 2: Field estimates of CH_4 dam degassing compared with ResME maximum potential degassing estimate (Gg CH_4-C/yr).

System	Annual degassing estimates from field measurements (Gg *CH_4-C* /yr)	Maximum potential degassing estimate from ResME (Gg *CH_4-C* /yr) *[estimate if including autochthonous POC input estimates]*
Tucurui	527 (Fearnside, 2002)	89 *[242]*
Balbina	65 (Kemenes et al., 2007)	24 *[37]*
Petit Saut	7.5 (Abril et al., 2005)	7 *[12]*
Batang Ai	0.55 (Soued and Prairie, 2020)	0.4 *[1]*

542 Note: *All reservoirs stratify in the summer and have turbine intakes below the thermocline.*

543

544

545 **4.4** Organic carbon burial

546 In addition to estimating CH_4 emissions from reservoir surfaces and dams, ResME can
547 also estimate organic carbon burial rates for comparison with field estimates to assess model
548 performance. We estimate organic carbon burial for each carbon type (B_i) as:

549 $$B_i = C_i - 2 \times P_i$$

550 Where C_i is the annual input of each carbon type, P_i is the estimated methanogenesis from that
551 carbon source, and the factor of 2 accounts for the fraction of organic carbon converted to CO_2
552 (ResME assumes 50% of decaying carbon is converted to CO_2). The median ResME-estimated
553 organic carbon burial, when excluding allochthonous POC input, was 197 gC m^{-2} yr^{-1} (and 646 if
554 including allochthonous POC). This estimate is close to the median burial estimate of 279 gC m^{-2}
555 yr^{-1} in a global compilation of field measurements from Mendonça et al., 2017 (Figure S5),
556 even though Mendonça et al., 2017 used a different set of reservoirs. The general agreement
557 between measured and ResME-modeled burial estimates is another indication that ResME results
558 reflect field conditions when excluding estimated allochthonous POC inputs.

559 **4.5** Potential CH_4 contributions from newly flooded biomass

560 Creating reservoirs involves flooding significant quantities of carbon, both above and
561 below ground, which can fuel elevated CH_4 emissions soon after reservoir creation (Abril et al.,
562 2005; Barros et al., 2011; Tremblay et al., 2005; Venkiteswaran et al., 2013). The potential
563 importance of this post-construction pulse of CH_4 has not yet been quantified because previous
564 efforts to estimate CH_4 emissions from reservoirs did not model emissions changes over time.
565 We estimate the relative importance of newly flooded carbon to reservoir CH_4 emissions using
566 ResME. We ran ResME with and without the flooded carbon pool. Results show that this
567 above-ground carbon can substantially increase the amount of CH_4 emitted from reservoir
568 surfaces in the first 10 years after reservoir creation (Figure S6). The change is most dramatic

for less productive systems where annual carbon inputs are smaller, with oligotrophic reservoirs seeing an average 690% increase in CH_4 emissions from above-ground carbon over a 10-year period (Figure S6). Conversely, eutrophic systems see only a 190% increase on average, because modeled CH_4 emissions are driven more by annual inputs of autochthonous carbon.

While the values presented above provide a first-order estimate of how much additional CH_4 young reservoirs may produce, they are preliminary estimates. Lack of field measurements for young reservoirs makes it difficult to determine how well ResME reproduces CH_4 emissions after reservoir construction. We found 8 studies (from reservoirs in South America, Canada, Eastern Europe, and Southeast Asia) with CH_4 emissions measurements within the first 10 years after reservoir creation, and compared them to ResME model predictions without allochthonous POC inputs (Figure S7). While ResME is able to reasonably predict change in CH_4 emissions over time from several of the reservoirs, more measurements are needed to characterize how well ResME performance for young reservoirs.

5.0 Sensitivity analysis

We conducted a sensitivity analysis to assess the relative importance of assumptions made about carbon input, methanogenesis, and CH_4 fate and transport. We individually increased input parameters by 5% and recorded the mean change in predicted CH_4 release across the 57 reservoir subset (Table 3). Since age varies across the reservoirs and age affects the relative impact of the decay parameters, we fixed reservoir age at 50 yrs for consistency. To study the model sensitivity to the decay parameters, we compared results for reservoirs at 1 year versus 50 years. Our results show that for the set of assumptions governing carbon input to reservoirs, ResME is most sensitive to changes in the dominant carbon source. When excluding allochthonous POC from the carbon inputs, increasing autochthonous carbon inputs by 5% raises mean modeled results by 3.3%.

Table 3: Sensitivity Analysis

596

Treatment	**Parameter or input**	**Mean change in predicted CH_4 release (%)** Excluding allochthonous POC *[estimate if including autochthonous POC input estimates]*
Factors affecting carbon input		
+ 5%	Q (average reservoir discharge)	0.01 *[1.0]*
+ 5%	R (basin relief)	0.8 *[2.2]*
+ 5%	Fraction of POC in total sediment load	1.5 *[3.5]*
+ 5%	Ratio of DOC to POC	2.4 *[0.5]*
+ 5%	Flocculation rate	1.5 *[0.3]*
+ 5%	Ratio of autochthonous input reaching the sediment	3.3 *[1.4]*
+ 5%	Autochthonous input	3.3 *[1.4]*
+ 5%	Flooded carbon input	0.2 *[0.04]*
+ 5%	Allochthonous POC input	na *[3.3]*
+ 5%	Allochthonous DOC input	1.5 *[0.6]*

Factors affecting methanogenesis			
+ 5%	Epilimnion temperature	1.3 *[1.3]*	
+ 5%	Hypolimnion temperature	1.1 *[1.1]*	
+ 5%	Ratio of epilimnion to hypolimnion area	0.3 *[0.3]*	
+ 5%	Flooded carbon *v* decay parameter	-0.09 *[-0.02]*	3.6 *[2.8]* *
+ 5%	Flooded carbon α decay parameter	0.06 *[0.01]*	-2.5 *[-2.0]* *
+ 5%	Autochthonous *v* decay parameter	2.5 *[1.0]*	0.3 *[0.2]* *
+ 5%	Autochthonous α parameter	-0.4 *[-0.2]*	-0.1 *[-0.1]* *
+ 5%	Allochthonous *v* decay parameter	1.2 *[2.7]*	0.2 *[1.2]* *
+ 5%	Allochthonous α decay parameter	-0.2 *[-0.5]*	-0.1 *[-0.6]* *
+ 5%	Ratio of CH_4 to CO_2 production	5.0 *[5.0]*	
Factors affecting internal fate/transport			
+ 5%	Baseline fraction of CH_4 production that gets internally oxidized or emitted via turbines (0.5 in Equation 6)	-6.5 *[-6.5]*	
+ 5%	Bubble dissolution rate	-1.5 *[-1.5]*	

+ 5%	Plant emissions (as % of eb + diff)	-4.8 *[-4.8]*

** Reservoir age fixed at 1 year instead of 50 years*

Note: Results of the sensitivity analysis where individual parameters or inputs were increased by 5%. Results show the mean change in predicted CH_4 ebullition and diffusion. Reservoir age fixed at 50 years, unless otherwise noted.

Of the parameters affecting methanogenesis rates, ResME is most sensitive to changing the *v* decay parameter, then to changing sediment temperatures, and lastly to changing α parameters for autochthonous and allocthonous carbon. When reservoir age is fixed at 50 years, a 5% increase in the *v* decay parameter for autochthonous carbon and allochthonous carbon yields a 2.5% and 1.2% increase in estimated ebullition plus diffusion (respectively, when excluding allochthonous POC). ResME is less sensitive to changing the α decay parameter, where a 5% increase in the α decay parameter for autochthonous and allochthonous carbon results in a -0.4%, and -0.2% change in emissions for each carbon source, respectively.

The effect of changing *v* and α for flooded carbon depends on the reservoir age, and the effect is larger when the reservoir is younger. Right after reservoir creation, increasing α (a proxy for average carbon lifetime) decreases CH_4 emissions in the short term, as flooded biomass carbon takes longer to break down. Conversely, raising *v* makes carbon less recalcitrant, which will increase CH_4 emissions. However, the effect changes when the reservoir is 50 years old. At 50 years, a higher α means there is more carbon left to decompose, so raising α raises average CH_4 emissions slightly. Raising *v* to make carbon less recalcitrant means more of the carbon will have decomposed at 50 years, thus lowering average CH_4 emissions.

Overall, ResME is most sensitive to changing the parameters governing CH_4 fate and transport within the reservoir, since these mechanisms act on CH_4 produced from all carbon types. ResME is most sensitive to a change in the baseline fraction (0.5, Equation 6) of produced CH_4 that gets internally oxidized or emitted via turbines (or immediately downstream of turbines), then to a change in the fraction of plant emissions, and finally to bubble dissolution.

Increasing all three of these parameters results in a decrease in estimated ebullition plus diffusion. For the case of increasing plant emissions, ebullition and diffusion decrease as more of the CH_4 is partitioned for plant release, so total reservoir emissions remain constant. Increasing the baseline internal oxidation results in decreased ebullition and diffusion emissions, but would increase potential turbine emissions for reservoirs with turbine intakes in hypolimnetic waters (because oxidation and turbine CH_4 release are directly and negatively coupled in ResME). Increasing bubble dissolution has a similar effect to increasing baseline internal oxidation, as CH_4 dissolved from bubbles is subject to oxidation or export through turbines.

Overall, the sensitivity test shows that ResME is reasonably robust against small changes in parameter input values. A 5% increase in parameter input value produces a 5% or smaller increase in surface CH_4 emissions estimates, for all input parameters except the baseline fraction of CH_4 production that gets internally oxidized. ResME is most sensitive to this parameter, yet a 5% change only yields a -6.5% change in estimated surface CH_4 emissions.

6.0 Global CH_4 Emissions from Hydroelectric Reservoirs

There are 2,462 hydropower reservoirs in the GRanD global database (Figure 4), and collectively these reservoirs represent approximately 287,000 km^2 of surface area. Previous studies have used empirical estimates of CH_4 production to estimate that these existing reservoirs may emit around 3 - 13.3 Tg CH_4-C per year (Li and Zhang, 2014; Barros et al., 2011).

We used ResME to estimate current global CH_4 emissions from hydropower reservoirs. We excluded allochthonous POC because model/data comparisons showed that allochthonous POC inputs bias ResME results (Figure 6). While detailed information about reservoir primary production rates is not available for all reservoirs in GRanD, recent work by Sayers *et al.* (2021) has shown that in-situ primary production in lakes and reservoirs is correlated with latitude. The Sayers relationship between latitude and carbon fixation produces lower values of carbon fixation than would be expected from field measurements in reservoir systems, which likely reflects that lakes typically have lower carbon fixation than reservoirs (Wetzel, 2001). To make the global Sayers *et al.* (2021) relationship more compatible with the field-based estimates of primary production specifically from reservoirs (ie: 2019 mg CH_4-C m^{-2} day^{-1} from eutrophic

systems), we increased the sensitivity in the Sayers relationship between primary production and latitude, such that the highest production systems averaged 2019 mg CH_4-C m^{-2} day^{-1} (compared with the Sayers value of 1279 mg CH_4-C m^{-2} day^{-1} which was derived with lake and reservoir data). We did this by increasing the northern hemisphere y-intercept between latitude and primary production from 1279 mg CH_4-C m^{-2} day^{-1} to 2019 mg CH_4-C m^{-2} day^{-1} (and the southern hemisphere intercept from 1227 to 2019 mg CH_4-C m^{-2} day^{-1}). We use this adjusted, latitude-based estimate of primary production in our "best" estimate of global hydropower CH_4 emissions. Given the additional uncertainties introduced with adjusting the Sayers *et al*. (2021) relationship, and the fact that Sayers *et al,* 2021 does not account for other factors affecting trophic status (such as nutrient loading), we also calculate lower and upper bounds for CH_4 emissions assuming all reservoirs are either oligotrophic or eutrophic, respectively.

Since estimating hypolimnetic sediment area versus epilimnetic sediment area was infeasible on the global scale, and our sensitivity analysis showed that ResME was relatively insensitive to changing the ratio of epilimnetic to hypolimnetic sediments, we assumed all sediment temperature was equivalent to the hypolimnetic sediment temperature (Equation S7).

We applied ResME to hydropower reservoirs from GRanD. Since 10 of the reservoirs account for 26% of the total surface area, we used literature estimates of reservoir trophic status to assign fixed values of primary production to these largest systems (Table S9). We then ran ResME to estimate global CH_4 emission from diffusion and bubbling, and the theoretical maximum emission from turbines (assuming all reservoir turbine intakes pull from the base of the hypolimnion). Following Deemer et al., 2016, we excluded Lakes Victoria, Baikal, and Ontario as these large systems are natural lakes modified with hydropower facilities.

Our simulation results show that existing hydropower facilities emit 4.3 Tg CH_4 - C yr^{-1} via ebullition, diffusion, and plants, when using the adjusted Sayers *et al*, 2021 relationship between primary production and latitude (and excluding allochthonous POC). Maximum potential emissions from turbine degassing were an additional 6.6 Tg CH_4- C yr^{-1}. Since not all reservoirs in GRanD have turbine intakes within the hypolimnion, the true global emissions from turbine outlets are likely lower. If we assume actual turbine degassing is 50% of the maximum estimated (we do not have estimates of turbine placements on a global scale), total global CH_4

emissions from hydropower reservoirs are 7.7 Tg CH_4– C yr^{-1}. We can estimate a lower bound on potential CH_4 emissions by assuming all reservoirs are oligotrophic, which yields 1 Tg CH_4– C yr^{-1} from surface emissions and 1.7 Tg CH_4– C yr^{-1} potential emissions from turbines. The upper bound (assuming all reservoirs are eutrophic) is 7.0 Tg CH_4– C yr^{-1} and 10.4 Tg CH_4– C yr^{-1} from dams (if all dams draw water from hypolimnion). We also note that hydropower reservoirs (excluding Lakes Victoria, Baikal, and Ontario) make up 82% of total reservoir surface area in GRanD, so global emissions from all reservoirs is higher than ResME estimates.

In addition to the uncertainty introduced by our assumptions about trophic status, the substantial spread between ResME results and field data indicates large additional uncertainty (Figure 6). This uncertainty likely results from the calculations and approximations used to parameterize ResME, and from the fact that relatively sparse field estimates lead to uncertain estimates of total reservoir emissions. Within the 57 reservoirs of the reservoir subset, mean ebullition and diffusion was 59 mg CH_4-C m^{-2} day^{-1}, and the mean residual was 280, or a factor of 4.7. If we apply a positive and negative factor of 4.7 to our global estimates, we estimate a range for global hydropower surface emissions of 0.9 – 20.1 Tg CH_4-C yr^{-1}.

The potential turbine sources are relatively large point sources. For example, 36% of reservoirs have maximum potential dam emissions higher than anthropogenic super-emitters, defined as sources exceeding 0.3 t CH_4/hr by Subramanian et al., 2015. (estimated assuming the annual turbine emissions occur over a 3-month period) (Figure 7). If all GRanD reservoirs were either oligotrophic or eutrophic, 24% or 41% would exceed 0.3 t/hr for all oligotrophic or all eutrophic systems (respectively). Table S10 contains a list of the top 20 CH_4 emitting reservoirs (based on turbine emissions), with estimations for maximum potential turbine emissions (both annual values, and values assuming all turbine emissions occur exclusively within a 3 month period) and surface emissions.

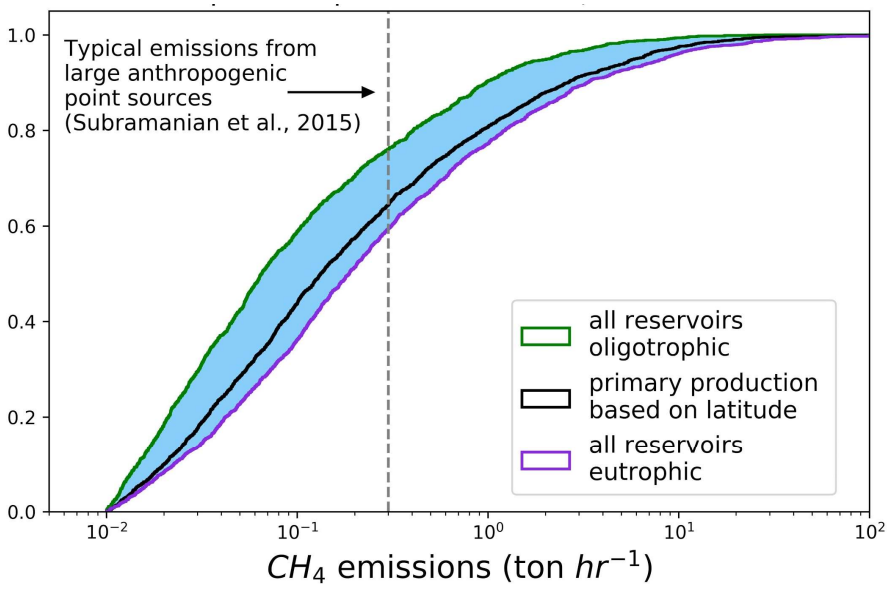

Figure 7: Cumulative frequency distributions for modeled maximum potential dam CH_4 emissions assuming GRanD reservoir trophic status is based on latitude (black line), assuming all reservoirs are oligotrophic (green line), or assuming all reservoirs are eutrophic (purple line). For comparison, the grey dashed line shows methane (CH_4) emissions from a large anthropogenic point source, defined as 0.3 t CH_4/hr (Subramanian et al., 2015).

Emissions from hydroelectric reservoirs can also dominate CH_4 emissions on local scales. We compared the estimated CH_4 hydropower emissions to all anthropogenic and natural CH_4 emissions used in the GEOS-Chem atmospheric chemistry model (Maasakkers et al., 2019; The International GEOS-Chem User Community, 2018). Emissions from hydropower reservoirs accounted for over 50% of total CH_4 emissions in 12 of the land (2° x 2.5°) grid cells (Figure S9) when primary production is based on latitude. Methane emissions from hydropower are more likely to dominate regional emissions in places like Canada, Brazil, sub-Saharan Africa, and Russia than in China or India which have high overall CH_4 emissions.

Our estimate of 4.3 Tg CH4-C yr^{-1} emitted from hydropower facilities falls within the range of previously estimated emissions from hydropower facilities (Barros et al., 2011; Li & Zhang, 2014). While previous estimates relied on data-fitting to measure emission rates, ResME is a mechanistic model with no empirically fitted parameters. The mechanistic basis of the

model allows for a deeper understanding of the factors affecting CH_4 emissions from hydropower. As our results have shown, estimated CH_4 emissions are particularly sensitive to the CH_4 fate and transport estimations that affect CH_4 produced from all carbon inputs. The model is much less sensitive to the α decay parameter (related to the average lifetime of the more reactive compounds) than to v (related to carbon recalcitrance). This type of insight is only possible from a mechanistic model and highlights the relative advantages of using ResME to estimate reservoir CH_4 emissions.

7.0 Future research needs to reduce uncertainty in emissions estimates

ResME represents an important step forward in reservoir emissions modeling because the mechanistic framework allows for a more detailed understanding of emissions drivers. However, ResME (as well as other empirical models of CH_4 emissions) have large uncertainties. While these uncertainties are to be expected in complex, dynamic ecosystems such as reservoirs, significant reductions in uncertainty would help better constrain the potential carbon benefits from hydroelectric power as well as CH_4 source-attribution in the global CH_4 budgets. Some keys to reducing ResME uncertainty are to improve allochthonous POC loading estimates, add turbine intake depth information, increase sampling frequency in field campaigns, increase studies of newly flooded reservoirs, and potentially use satellite CH_4 measurements to constrain turbine emissions.

As previously described, ResME-modeled CH_4 emissions from allochthonous POC inputs appear to be too high based on measured CH_4 emissions from the reservoir surface. ResME-modeled allochthonous POC input also results in estimated carbon burial that exceeds the typical range presented in the literature. This suggests that estimated inputs of allochthonous POC are too high, which is also indicated by the fact that ResME estimates of incoming river POC concentration are higher than the global distribution (although this difference could, at least in part, be because our reservoir subset is not necessarily representative of global rivers). Since

ResME estimates of allochthonous POC were built on published, data-verified methods (albeit methods with relatively high uncertainty) to estimate POC loading, more work is needed to determine why modeled CH_4 emissions from allochthonous POC are not supported by field data. Spatially-explicit sampling in reservoirs could help determine if allochthonous POC loading primarily occurs near river mouths, in which case field measurements ignoring river mouths could under-represent reservoir CH_4 production and at least partially explain the discrepancy when including allochthonous POC inputs.

Dam design (e.g., turbine intake depth) greatly influences potential turbine emissions, yet the GRanD database lacks information on the relative water intake height for each dam. Updating GRanD to contain this information would allow us to narrow the range of estimated CH_4 degassing at turbines. Additional studies to measure turbine degassing from deep-intake turbines would also help reduce the uncertainty around ResME estimates for turbine degassing, since we currently only have 4 studies measuring emissions from deep-intake turbines.

Uncertainty in the estimates of CH_4 emissions from hydropower reservoirs, particularly recently-flooded reservoirs, could be reduced through more robust field campaigns to accurately estimate surface emissions. A recent statistical analysis on the sampling necessary to adequately estimate CH_4 emissions found that diffusive and ebullitive fluxes should be measured for at least 11 or 39 days over at least 3 or 11 depth-stratified locations, respectively (Wik et al., 2016). Given the practical constraints on such extensive sampling, the large majority of studies do not attain this rigorous requirement. More extensive field campaigns could provide more accurate results, though such campaigns can be prohibitively time intensive. More field campaigns in newly flooded reservoirs are especially important given the potential for very large emissions from these systems, and the current lack of data from systems less than 10 years old.

Measured estimates of reservoir CH_4 emissions could also be improved through remote sensing data from satellites. The TROPOMI instrument launched in October 2017 provides global daily mapping of atmospheric CH_4 columns at 5.5 km x 7 km pixel resolution (Veefkind et al., 2012; Hasekamp et al., 2019). TROPOMI's theoretical point source detection threshold is about 4 t CH_4/hr (Jacob et al., 2016), and 39 of the 2459 GRanD reservoirs have annual average turbine emissions exceeding this threshold (assuming deep-intake turbines). Since the turbine

784 degassing flux is likely concentrated in the warm months when reservoirs are stratified, we
785 assume annual turbine emissions occur over a 3-month period, and then 184 of the GRanD
786 reservoirs could exceed TROPOMI's CH_4 detection threshold. However, TROPOMI and other
787 satellites cannot measure CH_4 concentrations over water except for with sunglint, and
788 TROPOMI's coverage is limited by clouds, topography, aerosol, and inhomogeneous surface
789 reflectances. Despite these limitations, initial attempts to find turbine-related CH_4 plumes in
790 TROPOMI yielded promising results near the Lom Pangar dam in Cameroon. Figure 8 shows
791 two days in December with a clear CH_4 enhancement over the dam. Sentinel-2 visual imagery
792 from December 25 shows that water is flowing through the dam during that time period (Gascon
793 et al. 2017). The GHGSat satellite instrument targeted at point source observations has a 0.05
794 km x 0.05 km pixel size and a lower detection threshold at 0.25 t CH_4/hr (meaning GHGSat can
795 detect weaker sources of CH_4), and was also able to detect a CH_4 plume from turbine outgassing
796 over the Lom Pangar dam (Struple et al. 2019). Assuming turbine emissions are concentrated in
797 3 summer months, 38% of the GRanD reservoirs could have turbine fluxes detectable by
798 GHGSat (if turbines pull from a CH_4-rich hypolimnion). We also note that data from the
799 Airborne Visible Infrared Imaging Spectrometer (AVIRIS) taken over water with high sun glint
800 have been used to estimate CH_4 emissions over water, though these measurements are not
801 available globally (Thorpe et al., 2013).

802

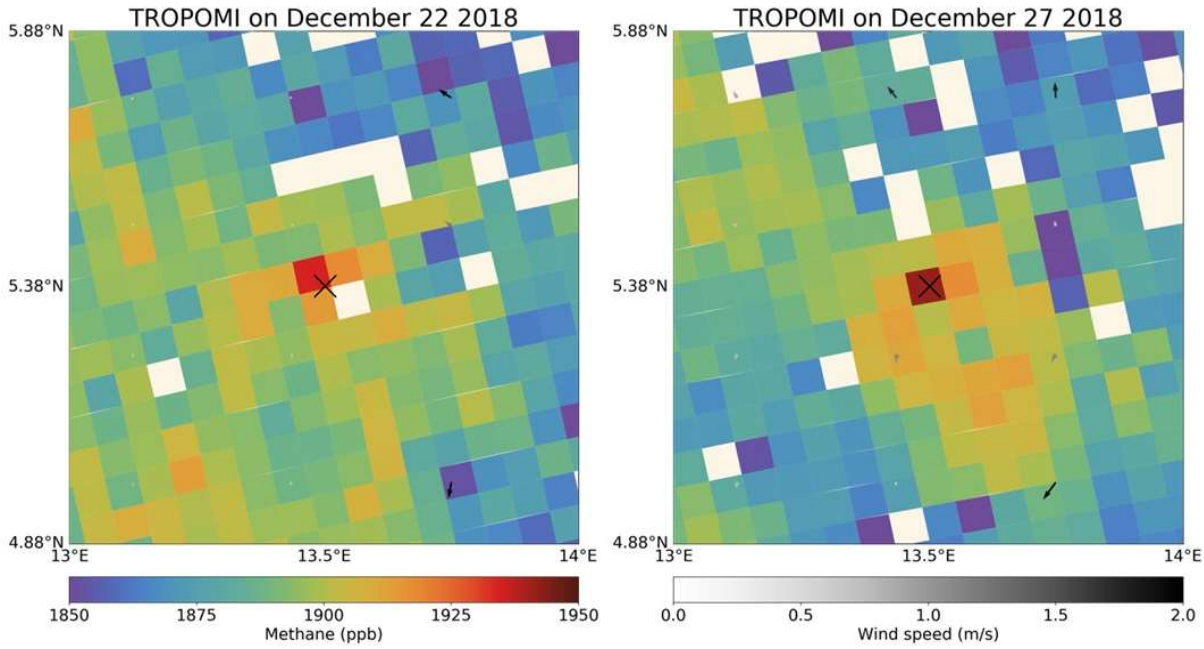

Figure 8: TROPOMI methane data show an enhancement over the Lom Pangar dam (indicated by the cross) in Cameroon in December 2018. Also shown are 10m wind vectors from the GEOS-FP reanalysis product (Molod et al., 2012).

7.0 Conclusions

Our estimate of 4.3 Tg CH_4-C yr^{-1} emitted from hydropower reservoir surfaces falls within the range of previously estimated emissions from hydropower facilities (Barros et al., 2011; Li & Zhang, 2014). However, large uncertainties remain, with ResME global uncertainty producing a range of 0.9 – 20.1 Tg CH_4-C yr^{-1}, and significant work will be needed to reduce this uncertainty. The additional maximum contribution of 6.6 Tg CH4-C yr^{-1} from turbine outflows (assuming all turbines have deep water intakes) shows that turbine outflows contribute substantially to total reservoir CH_4 emissions.

Contributions from newly flooded carbon can substantially increase CH_4 emissions in the few years after reservoir creation, though more field measurements are needed to reduce uncertainty. Improving estimates for newly flooded reservoirs will be particularly important in the future, since there were 3,700 new hydropower dams planned as of 2015 (Zarfl et al., 2015).

Predicting, and potentially mitigating, the CH_4 emissions from these new systems will require more detailed data describing how CH_4 emissions evolve after reservoir creation.

While previous estimates relied on data-fitting to measure emission rates, ResME is a mechanistic model with no empirically fitted parameters. The mechanistic basis of the model allows for a deeper understanding of the factors affecting CH_4 emissions from hydropower. As our results have shown, estimated CH_4 emissions are particularly sensitive to estimates in carbon loading and the decay parameters used to estimate methanogenesis rates. The model is comparatively insensitive to changes in sediment temperature. This type of insight is only possible from a mechanistic model, and highlights the relative advantages of using ResME to estimate reservoir CH_4 emissions. This mechanistic understanding will continue to be important as hydropower expands globally.

Data Availability

Global CH_4 emissions estimates from hydropower are provided in 2 NetCDF files at http://doi.org/10.5281/zenodo.4730937 (Delwiche et al., 2021). Emissions are divided into reservoir surface emissions and potential dam emissions, and are provided for 0.1 x 0.1 pixels. Reservoir surface emissions are evenly distributed over the grid cells containing the reservoir footprint (footprint information from GRanD) and are given in kg m^{-2} s^{-1}. Potential dam emissions are assigned to the grid cell containing the dam coordinates from GRanD.

Model files necessary for estimating CH_4 emissions from the subset of reservoirs used in this text are provided at https://github.com/kylebdelwiche/ResMe. TROPOMI data are available at https://s5phub.copernicus.eu/. GEOS-FP data are available at https://gmao.gsfc.nasa.gov/GMAO_products/. Sentinel- 2 data are available from the Copernicus Open Access Hub (https://scihub.copernicus.eu), and data used here was obtained from the Sentinel Hub EO Browser (apps.sentinel-hub.com/eo-browser/).

Acknowledgements

This work was supported by the Harvard Climate Change Solutions fund and the NASA Carbon Monitoring System. We acknowledge support from the Gordon and Betty Moore Foundation (Grant GBMF5439, "Advancing Understanding of the Global Methane Cycle"; Stanford University). Part of this research was carried out at the Jet Propulsion Laboratory, California Institute of Technology, under a contract with the National Aeronautics and Space Administration. The authors thank the team that realized the TROPOMI instrument and its data products, consisting of the partnership between Airbus Defence and Space Netherlands, KNMI, SRON, and TNO, commissioned by NSO and ESA. Sentinel-5 Precursor is part of the EU Copernicus program, and Copernicus (modified) Sentinel-5P data (2018) have been used.

References

Abril, G., Guérin, F., Richard, S., Delmas, R., Galy-Lacaux, C., Gosse, P., Tremblay, A., Varfalvy, L., et al. (2005). Carbon dioxide and methane emissions and the carbon budget of a 10-year old tropical reservoir (Petit Saut, French Guiana). *Global Biogeochemical Cycles*, *19*(4). https://doi.org/10.1029/2005GB002457.

Almeida, R. M., Nóbrega, G. N., Junger, P. C., Figueiredo, A. V., Andrade, A. S., de Moura, C. G. B., Tonetta, D., Oliveira, E. S., et al. (2016). High Primary Production Contrasts with Intense Carbon Emission in a Eutrophic Tropical Reservoir. Frontiers in Microbiology, *7*. https://doi.org/10.3389/fmicb.2016.00717.

Alves, B. G. T. A. & Bertolino, S. M. (2016). Estudo du grau de trofia da represa de Miranda-mg. XIII Congresso Nacional de Meio Ambiente de Pocos de Caldas.

Barros, N., Cole, J. J., Tranvik, L. J., Prairie, Y. T., Bastviken, D., Huszar, V. L. M., del Giorgio, P., & Roland, F. (2011). Carbon emission from hydroelectric reservoirs linked to reservoir age and latitude. *Nature Geoscience*, *4*(9), 593–596. https://doi.org/10.1038/ngeo1211.

Bastviken, D., Cole, J. J., Pace, M. L., & Van de Bogert, M. C. (2008). Fates of methane from different lake habitats: Connecting whole-lake budgets and CH4 emissions. Journal of Geophysical Research: Biogeosciences, 113(G2). https://doi.org/10.1029/2007JG000608.

Bastviken, D., Tranvik, L. J., Downing, J. A., Crill, P. M., & Enrich-Prast, A. (2011). Freshwater methane emissions offset the continental carbon sink. *Science*, *331*(6013), 50. https://doi:10.1126/science.1196808.

Beaulieu, J. J., Smolenski, R. L., Nietch, C. T., Townsend-Small, A., & Elovitz, M. S. (2014). High methane emissions from a midlatitude reservoir draining an agricultural watershed. *Environmental Science & Technology*, *48*(19), 11100–11108. https://doi.org/10.1021/es501871g.

Beusen, A. H. W., Dekkers, A. L. M., Bouwman, A. F., Ludwig, W., & Harrison, J. (2005). Estimation of global river transport of sediments and associated particulate C, N, and P. Global Biogeochemical Cycles, 19(4). https://doi.org/10.1029/2005GB002453.

Bižić-Ionescu, M., Klintzsch, T., Ionescu, D., Hindiyeh, M. Y., Günthel, M., Muro-Pastor, A. M., Eckert, W., Keppler, F., & Grossart, H.-P. (2020). Widespread methane formation by Cyanobacteria in aquatic and terrestrial ecosystems. *Science Advances, 6*(3). https://doi.org/10.1126/sciadv.aax5343.

Bogard, M. J., del Giorgio, P. A., Boutet, L., Chaves, M. C. G., Prairie, Y. T., Merante, A., & Derry, A. M. (2014). Oxic water column methanogenesis as a major component of aquatic CH4 fluxes. *Nature Communications*, *5*(1), 5350. https://doi.org/10.1038/ncomms6350.

Borrel, G., Jézéquel, D., Biderre-Petit, C., Morel-Desrosiers, N., Morel, J.-P., Peyret, P., Fonty, G., & Lehours, A.-C. (2011). Production and consumption of methane in freshwater lake ecosystems. Research in Microbiology, 162(9), 832–847. https://doi:10.1016/j.resmic.2011.06.004.

Boudreau, B. P., & Ruddick, B. R. (1991). On a reactive continuum representation of organic matter diagenesis. *American Journal of Science*, *291*(5), 507–538. https://doi.org/10.2475/ajs.291.5.507.

Boudreau, B. P., Arnosti, C., Jørgensen, B. B., & Canfield, D. E. (2008). Comment on" Physical model for the decay and preservation of marine organic carbon." *Science*, *319*(5870), 1616–1616. https://doi.org/10.1126/science.1148589.

Boylan, J. W., & Russell, A. G. (2006). PM and light extinction model performance metrics, goals, and criteria for three-dimensional air quality models. *Atmospheric Environment*, *40*(26), 4946–4959. https://doi.org/10.1016/j.atmosenv.2005.09.087.

Casper, P., Maberly, S. C., Hall, G. H., & Finlay, B. J. (2000). Fluxes of methane and carbon dioxide from a small productive lake to the atmosphere. Biogeochemistry, 49(1), 1–19. https://doi.org/10.1023/A:1006269900174.

Catalan N., Casas-Ruiz, J.P., von Schiller, D., Proia, L., Obrador, B., Zwirnmann, E., & Marce, R. (2017). Biodegradation kinetics of dissolved organic matter chromatographic fractions in an intermittent river. *Journal of Geophysical Research: Biogeosciences, 122,* 131-144. https://doi.org/10.1002/2016JG003512.

Chanudet, V., Descloux, S., Harby, A., Sundt, H., Hansen, B. H., Brakstad, O., Serça, D., & Guerin, F. (2011). Gross CO2 and CH4 emissions from the Nam Ngum and Nam Leuk sub-tropical reservoirs in Lao PDR. *Science of The Total Environment, 409*(24), 5382–5391. https://doi.org/10.1016/j.scitotenv.2011.09.018.

Conrad, R. (2005). Quantification of methanogenic pathways using stable carbon isotopic signatures: a review and a proposal. *Organic geochemistry, 36,* 739-752. https://doi.org/10.1016/j.orggeochem.2004.09.006.

Conrad, R., Klose, M., Claus, P., & Enrich-Prast, A. (2010). Methanogenic pathway, 13C isotope fractionation, and archaeal community composition in the sediment of two clear-water lakes of Amazonia. *Limnology and Oceanography*, *55*(2), 689–702. https://doi.org/10.4319/lo.2010.55.2.0689.

Deemer, B. R., Harrison, J. A., Li, S., Beaulieu, J. J., DelSontro, T., Barros, N., Bezerra-Neto, J. F., Powers, S. et al. (2016). Greenhouse Gas Emissions from Reservoir Water Surfaces: A New Global Synthesis. *Bioscience*, *66*(11), 949–964. https://doi.org/10.1093/biosci/biw117.

DelSontro, T., Kunz, M. J., Kempter, T., Wüest, A., Wehrli, B., & Senn, D. B. (2011). Spatial heterogeneity of methane ebullition in a large tropical reservoir. *Environmental Science & Technology*, *45*(23), 9866–9873. https://doi.org/10.1021/es2005545.

DelSontro, T., McGinnis, D. F., Wehrli, B., & Ostrovsky, I. (2015). Size does matter: importance of large bubbles and small-scale hot spots for methane transport. *Environmental Science & Technology*, *49*(3), 1268–1276. https://doi.org/10.1021/es5054286.

DelSontro, T., Beaulieu, J. J., & Downing, J. A. (2019). Greenhouse gas emissions from lakes and impoundments: upscaling in the face of global change. *Limnology and Oceanography Letters*, *3*(3), 64–75. https://doi.org/10.1002/lol2.10073.

Delwiche, K. B., & Hemond, H. F. (2017). Methane Bubble Size Distributions, Flux, and Dissolution in a Freshwater Lake. *Environmental Science & Technology*, *51*(23), 13733–13739. https://doi.org/10.1021/acs.est.7b04243.

Delwiche, K.B., Harrison, J. A., Maasakkers, J. D., Sulprizio, M. P., Worden, J., Jacob, D. J., & Sunderland, E. M. (2021). ResME - A Global Mechanistic Model for Methane Emissions from Hydroelectric Reservoirs (gridded methane emissions data for reservoir surfaces and maximum potential dam emissions) [Data set]. Zenodo. http://doi.org/10.5281/zenodo.4730937.

Etminan, M., Myhre, G., Highwood, E. J., & Shine, K. P. (2016). Radiative forcing of carbon dioxide, methane, and nitrous oxide: A significant revision of the methane radiative forcing. *Geophysical Research Letters, 43*(24), 12,614–12,623. https://doi.org/10.1002/2016gl071930.

Fearnside, P. M. (2002). Greenhouse gas emissions from a hydroelectric reservoir (Brazil's Tucurui dam) and the energy policy implications. *Water, Air, and Soil Pollution*, *133*, 69–96. https://doi.org/10.1023/A:1012971715668.

Fernández, E. J., Peeters, F., & Hofmann, H. (2014). Importance of the autumn overturn and anoxic conditions in the hypolimnion for the annual methane emissions from a temperate lake. *Environmental Science & Technology, 48*(13), 7297–7304. https://doi.org/10.1021/es4056164.

Gascon, F., Bouzinac, C., Thépaut, O., Jung, M., Francesconi, B., Louis, J., Lonjou, V., Lafrance, B., Massera, S., Gaudel-Vacaresse, A., et al., 2017. Copernicus sentinel-2a calibration and products validation status. *Remote Sensing 9*, 584. https://doi.org/10.3390/rs9060584.

Grinham, A., Dunbabin, M., Gale, D., & Udy, J. (2011). Quantification of ebullitive and diffusive methane release to atmosphere from a water storage. *Atmospheric Environment*, *45*(39), 7166–7173. https://doi.org/10.1016/j.atmosenv.2011.09.011.

Grossart, H.-P., Frindte, K., Dziallas, C., Eckert, W., & Tang, K. W. (2011). Microbial methane production in oxygenated water column of an oligotrophic lake. *Proceedings of the National*

Academy of Sciences of the United States of America, *108*(49), 19657–19661. https://doi.org/10.1073/pnas.1110716108.

Gudasz, C., Bastviken, D., Premke, K., Steger, K., & Tranvik, L. J. (2012). Constrained microbial processing of allochthonous organic carbon in boreal lake sediments. *Limnology and Oceanography*, *57*(1), 163–175. https://doi.org/10.4319/lo.2012.57.1.0163.

Günthel, M., Donis, D., Kirillin, G., Ionescu, D., Bizic, M., McGinnis, D. F., Grossart, H.-P., & Tang, K. W. (2019). Contribution of oxic methane production to surface methane emission in lakes and its global importance. Nature Communications, 10(1). https://doi.org/10.1038/s41467-019-13320-0

Hall, B. D., & St Louis, V. L. (2004). Methylmercury and total mercury in plant litter decomposing in upland forests and flooded landscapes. *Environmental Science & Technology*, *38*(19), 5010–5021. https://doi.org/10.1021/es049800q.

Harfmann, J. L., Guillemette, F., Kaiser, K., Spencer, R. G. M., Chuang, C., & Hernes, P. J. (2019). Convergence of Terrestrial Dissolved Organic Matter Composition and the Role of Microbial Buffering in Aquatic Ecosystems. *Journal of Geophysical Research: Biogeosciences*, *124*(10), 3125–3142. https://doi.org/10.1029/2018JG004997.

Hasekamp, O., Lorente, A., Hu, H., Butz, A., Aan de Brugh, J., & Landgraf, J. (2019). Algorithm Theoretical Baseline Document for Sentinel-5 Precursor Methane Retrieval (SRON-S5P-LEV2-RP-001, 2019). https://sentinel.esa.int/documents/247904/2476257/Sentinel-5P-TROPOMI-ATBD-Methane-retrieval.

International Energy Agency. (2018). *World Energy Balances 2018*. OECD.

Jacob, D. J., Turner, A. J., Maasakkers, J. D., Sheng, J., Sun, K., Liu, X., Chance, K., Aben, I., McKeever, J., & Frankenberg, C. (2016). Satellite observations of atmospheric methane and their value for quantifying methane emissions. Atmospheric Chemistry and Physics, 16(22), 14371–14396. https://doi.org/10.5194/acp-16-14371-2016.

Jansson, M., Persson, L., De Roos, A. M., Jones, R. I., & Tranvik, L. J. (2007). Terrestrial carbon and intraspecific size-variation shape lake ecosystems. *Trends in Ecology & Evolution*, *22*(6), 316–322. https://doi.org/10.1016/j.tree.2007.02.015.

Jones, R. I. (1992). The influence of humic substances on lacustrine planktonic food chains. *Hydrobiologia*, *229*(1), 73–91. https://doi.org/10.1007/BF00006992.

Kankaala, P., Taipale, S., Nykänen, H., & Jones, R. I. (2007). Oxidation, efflux, and isotopic fractionation of methane during autumnal turnover in a polyhumic, boreal lake. *Journal of Geophysical Research, 112*(G2). https://doi.org/10.1029/2006jg000336.

Kemenes, A., Forsberg, B. R., & Melack, J. M. (2007). Methane release below a tropical hydroelectric dam. *Geophysical Research Letters*, *34*(12), GB4007. https://doi.org/10.1029/2007GL029479.

Kessler, M. A., Plug, L. J., & Walter Anthony, K. M. (2012). Simulating the decadal- to millennial-scale dynamics of morphology and sequestered carbon mobilization of two thermokarst lakes in NW Alaska. *Journal of Geophysical Research: Biogeosciences, 117*(G2). https://doi.org/10.1029/2011jg001796.

Kimmel, B. L., Lind, O. T., & Paulson, L. J. (1990). Reservoir primary production. *In* K. W. Thornton, B. K. Kimmel, and F. E. Payne, eds. Reservoir Limnology: Ecological Perspectives. John Wiley & Sons, New York. pp. 133-193.

Koehler, B., von Wachenfeldt, E., Kothawala, D., & Tranvik, L. J. (2012). Reactivity continuum of dissolved organic carbon decomposition in lake wate r. *Journal of Geophysical Research*, *117*(G1), 141. https://doi.org/10.1029/2011JG001793.

Koehler, B., & Tranvik, L. J. (2015). Reactivity continuum modeling of leaf, root, and wood decomposition across biomes. *Journal of Geophysical Research: Biogeosciences*, *120*(7), 1196–1214. https://doi.org/10.1002/2015JG002908.

Lee, H., Chung, S., Ryu, I., & Choi, J. (2013). Three-dimensional modeling of thermal stratification of a deep and dendritic reservoir using ELCOM model. *Journal of Hydro-Environment Research*, *7*(2), 124–133. https://doi.org/10.1016/j.jher.2012.10.002.

Lehner, B., Liermann, C. Reidy, Revenga, C., Vörösmarty, C., Fekete, B., Crouzet, P., Döll, P., Endejan, M., Frenken, K., Magome, J., Nilsson, C., Robertson, J.C., Rodel, R., Sindorf, N., and Wisser, D. (2011). High-resolution mapping of the world's reservoirs and dams for sustainable river-flow management. Frontiers in Ecology and the Environment, 9 (9): 494-502. https://doi.org/10.1890/100125.

Li, S., & Zhang, Q. (2014). Carbon emission from global hydroelectric reservoirs revisited. *Environmental Science and Pollution Research International*, *21*(23), 13636–13641. https://doi.org/10.1007/s11356-014-3165-4.

Likens, G. E. (1975). Primary Production of Inland Aquatic Ecosystems. In R. W. Helmut Lieth (Ed.), *Primary Productivity of the Biosphere* (pp. 186–202). Springer-Verlag.

Ludwig, W., Probst, J.-L., & Kempe, S. (1996). Predicting the oceanic input of organic carbon by continental erosion. *Global Biogeochemical Cycles*, *10*(1), 23–41. https://doi.org/10.1029/95GB02925.

Maasakkers, J.D., Jacob, D.J., Sulprizio, M.P., Scarpelli, T., Nesser, H., Sheng, J.-X., Zhang, Y., Hersher, M., Bloom, A.A., Bowman, K.W., Worden, J.R., Janssens-Maenhout, G., and Parker, R.J. (2019). Global distribution of methane emissions, emission trends, and OH concentrations and trends inferred from an inversion of GOSAT satellite data for 2010-2015, Atmospheric Chemistry and Physics, 19, 7859-7881. https://doi.org/10.5194/acp-19-7859-2019.

Maeck, A., Delsontro, T., McGinnis, D. F., Fischer, H., Flury, S., Schmidt, M., Fietzek, P., & Lorke, A. (2013). Sediment trapping by dams creates methane emission hot spots. *Environmental Science & Technology*, *47*(15), 8130–8137. https://doi.org/10.1021/es4003907.

Mayr, M. G., Zimmermann, M., Dey, J., Brand, A., Wehrli, B., & Bürgmann, H. (2020). Growth and rapid succession of methanotrophs effectively limit methane release during lake overturn. *Communications Biology, 3*(108). https://doi.org/10.1038/s42003-020-0838-z.

McGinnis, D. F., Greinert, J., Artemov, Y., Beaubien, S. E., & Wüest, A. (2006). Fate of rising methane bubbles in stratified waters: How much methane reaches the atmosphere? *Journal of Geophysical Research*, *111*(C9). https://doi.org/10.1029/2005jc003183.

Mendonça, R., Müller, R. A., Clow, D., Verpoorter, C., Raymond, P., Tranvik, L. J., & Sobek, S. (2017). Organic carbon burial in global lakes and reservoirs. Nature Communications, 8(1), 1694. https://doi.org/10.1038/s41467-017-01789-6

Meybeck, M. (1982). Carbon, nitrogen, and phosphorus transport by world rivers. *American Journal of Science*, *282*(4), 401–450. https://doi.org/10.2475/ajs.282.4.401.

Meybeck, M., & Ragu, A. (2012). GEMS-GLORI world river discharge database. Laboratoire de Géologie Appliquée, Université Pierre et Marie Curie, Paris, France, PANGAEA, https://doi.org/10.1594/PANGAEA.804574.

Molod, A., Takacs, L., Suarez, M., Bacmeister, J., In-Sun, S., & Eichmann, A. (2012). The GEOS-5 Atmospheric General Circulation Model: Mean Climate and Development from

MERRA to Fortuna (Technical Report Series on Global Modeling and Data Assimilation, Volume 28, 2012).

Moran, M. A., Benner, R., & Hodson, R. E. (1989). Kinetics of microbial degradation of vascular plant material in two wetland ecosystems. *Oecologia*, *79*(2), 158–167. https://doi.org/10.1007/BF00388472.

Mostovaya, A., Hawkes, J. A., Koehler, B., Dittmar, T., & Tranvik, L. J. (2017). Emergence of the Reactivity Continuum of Organic Matter from Kinetics of a Multitude of Individual Molecular Constituents. *Environmental Science & Technology*, *51*(20), 11571–11579. https://doi.org/10.1021/acs.est.7b02876.

Musenze, R. S., Grinham, A., Werner, U., Gale, D., Sturm, K., Udy, J., & Yuan, Z. (2014). Assessing the spatial and temporal variability of diffusive methane and nitrous oxide emissions from subtropical freshwater reservoirs. *Environmental Science & Technology*, *48*(24), 14499–14507. https://doi.org/10.1021/es505324h.

Noori, R., Asadi, N., & Deng, Z. (2019). A simple model for simulation of reservoir stratification. Journal of Hydraulic Research, 57(4), 561–572. https://doi.org/10.1080/00221686.2018.1499052.

Ostrovsky, I., McGinnis, D. F., Lapidus, L., & Eckert, W. (2008). Quantifying gas ebullition with echosounder: the role of methane transport by bubbles in a medium-sized lake: Measuring methane transport with bubbles. Limnology and Oceanography, Methods, 6(2), 105–118. https://doi.org/10.4319/lom.2008.6.105.

Ostrovsky, I., & Yacobi, Y. Z. (2010). Sedimentation flux in a large subtropical lake: Spatiotemporal variations and relation to primary productivity. *Limnology and Oceanography*, *55*(5), 1918–1931. https://doi.org/10.4319/lo.2010.55.5.1918.

Prairie YT, Alm J, Harby A, Mercier-Blais S, Nahas R. (2017). The GHG Reservoir Tool (Gres) Technical documentation, UNESCO/IHA research project on the GHG status of freshwater reservoirs. Version 1.13. Joint Publication of the UNESCO Chair in Global Environmental Change and the International Hydropower Association, 1.13.

Sayers, M. J., Fahnenstiel, G. L., Shuchman, R. A. & Bosse, K. R. (2021). A new method to estimate global freshwater phytoplankton carbon fixation using satellite remote sensing: initial results. *International Journal of Remote Sensing, 42*(10), 3708-3730, https://doi.org/10.1080/01431161.2021.1880661.

Schaefer, K., James Collatz, G., Tans, P., Scott Denning, A., Baker, I., Berry, J., Prihodko, L., Suits, N., et al. (2008). Combined Simple Biosphere/Carnegie-Ames-Stanford Approach terrestrial carbon cycle model. Journal of Geophysical Research*, 113*(G3). https://doi.org/10.1029/2007jg000603

Schmid, M., Ostrovsky, I., & McGinnis, D. F. (2017). Role of gas ebullition in the methane budget of a deep subtropical lake: what can we learn from process-based modeling? Limnology and Oceanography, 62(6), 2674–2698. https://doi.org/10.1002/lno.10598.

Schubert, C. J., Diem, T., & Eugster, W. (2012). Methane Emissions from a Small Wind Shielded Lake Determined by Eddy Covariance, Flux Chambers, Anchored Funnels, and Boundary Model Calculations: A Comparison. *Environmental Science & Technology, 46*(8), 4515–4522. https://doi.org/10.1021/es203465x.

Sharma, S., Jackson, D. A., Minns, C. K., & Shuter, B. J. (2007). Will northern fish populations be in hot water because of climate change? Global Change Biology, 13(10), 2052–2064. https://doi.org/10.1111/j.1365-2486.2007.01426.x.

Soued, C., & Prairie, Y. T. (2020). The carbon footprint of a Malaysian tropical reservoir: measured versus modelled estimates highlight the underestimated key role of downstream processes. Biogeosciences , 17(2), 515–527. https://doi.org/10.5194/bg-17-515-2020.

Strupler, M., Jervis, D., McKeever, J., Gains, D., Varon, D., & Germain, S. (2019). Satellite Retrievals of Industrial Methane Emissions at High Resolution with GHGSat-D. Geophysical Research Abstracts, 21.

Subramanian, R., Williams, L. L., Vaughn, T. L., Zimmerle, D., Roscioli, J. R., Herndon, S. C., Yacovitch, T. I., Floerchinger, C., Tkacik, D. S., Mitchell, A. L., & Others. (2015). Methane emissions from natural gas compressor stations in the transmission and storage sector: Measurements and comparisons with the EPA greenhouse gas reporting program protocol. *Environmental Science & Technology, 49*(5), 3252–3261. https://doi.org/10.1021/es5060258.

Syvitski, J. P. M., Peckham, S. D., Hilberman, R., & Mulder, T. (2003). Predicting the terrestrial flux of sediment to the global ocean: a planetary perspective. *Sedimentary Geology*, *162*(1), 5–24. https://doi.org/10.1016/S0037-0738(03)00232-X.

Teodoru, C. R., Del Giorgio, P. A., Prairie, Y. T., & St-Pierre, A. (2013). Depositional fluxes and sources of particulate carbon and nitrogen in natural lakes and a young boreal reservoir in

Northern Québec. Biogeochemistry, 113(1-3), 323–339. https://doi.org/10.1007/s10533-012-9760-x.

The International GEOS-Chem User Community: geoschem/geos-chem: GEOS-Chem 12.1.1 (Version 12.1.1), Zenodo, https://doi.org/10.5281/zenodo.2249246, 13 December 2018.

Thorpe, A. K., Roberts, D. A., Bradley, E. S., Funk, C. C., Dennison, P. E., & Leifer, I. (2013). High resolution mapping of methane emissions from marine and terrestrial sources using a Cluster-Tuned Matched Filter technique and imaging spectrometry. Remote Sensing of Environment, 134, 305–318. https://doi.org/10.1016/j.rse.2013.03.018.

Tremblay A., L. Varfalvy C., Roehm M., Garneau (Ed.). (2005). Greenhouse Gas Emissions - Fluxes and Processes. Springer Berlin Heidelberg New York.

Utsumi, M., Nojiri, Y., Nakamura, T., Nozawa, T., Otsuki, A., Takamura, N., Watanabe, M., & Seki, H. (1998). Dynamics of dissolved methane and methane oxidation in dimictic Lake Nojiri during winter. *Limnology and Oceanography, 43*(1), 10–17. https://doi.org/10.4319/lo.1998.43.1.0010

Vachon, D., Prairie, Y. T., Guillemette, F., & Del Giorgio, P. A. (2017). Modeling allochthonous dissolved organic carbon mineralization under variable hydrologic regimes in boreal lakes. Ecosystems, 20(4), 781–795. https://doi.org/10.1007/s10021-016-0057-0.

Van Coillie, R., Visser, S. A., Campbell, P. G. C., & Jones, H. G. (1983). A study of the breakdown of wood of conifers submerged for over half a century in a reservoir. Annales de Limnologie, 19(2), 129-134. https://doi.org/10.1051/limn/1983014.

Veefkind, J. P., Aben, I., McMullan, K., Förster, H., de Vries, J., Otter, G., et al. (2012). TROPOMI on the ESA Sentinel-5 Precursor: A GMES mission for global observations of the atmospheric composition for climate, air quality and ozone layer applications. *Remote Sens. Environ*., 120, 70–83. https://doi.org/10.1016/j.rse.2011.09.027.

Venkiteswaran, J. J., Wassenaar, L. I., & Schiff, S. L. (2007). Dynamics of dissolved oxygen isotopic ratios: a transient model to quantify primary production, community respiration, and air–water exchange in aquatic ecosystems. Oecologia, 153(2), 385–398. https://doi.org/10.1007/s00442-007-0744-9.

Venkiteswaran, J. J., Schiff, S. L., St. Louis, V. L., Matthews, C. J. D., Boudreau, N. M., Joyce, E. M., Beaty, K. G., & Andrew Bodaly, R. (2013). Processes affecting greenhouse gas

production in experimental boreal reservoirs. Global Biogeochemical Cycles, 27(2). https://doi.org/10.1002/gbc.20046.

Wachenfeldt, E. von, Bastviken, D., & Tranvika, L. J. (2009). Microbially induced flocculation of allochthonous dissolved organic carbon in lakes. Limnology and Oceanography, 54(5), 1811–1818. https://doi.org/10.4319/lo.2009.54.5.1811.

Walter, K. M., Zimov, S. A., Chanton, J. P., Verbyla, D., & Chapin, F. S., 3rd. (2006). Methane bubbling from Siberian thaw lakes as a positive feedback to climate warming. *Nature*, *443*(7107), 71–75. https://doi.org/10.1038/nature05040.

West, W. E., Creamer, K. P., & Jones, S. E. (2016). Productivity and depth regulate lake contributions to atmospheric methane. Limnology and Oceanography, 61(S1), S51–S61. https://doi.org/10.1002/lno.10247.

Wetzel, R. (2001). *Limnology: Lake and River Ecosystems* (Vol. 3). San Diego, California, Academic Press.

Wik, M., Thornton, B. F., Bastviken, D., Uhlbäck, J., & Crill, P. M. (2016). Biased sampling of methane release from northern lakes: A problem for extrapolation. Geophysical Research Letters, 43(3), 1256–1262. https://doi.org/10.1002/2015gl066501.

Yao, M., Henny, C., & Maresca, J. A. (2016). Freshwater Bacteria Release Methane as a By-Product of Phosphorus Acquisition. Applied and Environmental Microbiology, 82(23), 6994–7003. https://doi.org/10.1128/AEM.02399-16.

Yigzaw, W., Li, H.-Y., Fang, X., Leung, L. R., Voisin, N., Hejazi, M. I., & Demissie, Y. (2019). A Multilayer Reservoir Thermal Stratification Module for Earth System Models. Journal of Advances in Modeling Earth Systems, 11(10), 3265–3283. https://doi.org/10.1029/2019MS001632.

Zarfl, C., Lumsdon, A. E., Berlekamp, J., Tydecks, L., & Tockner, K. (2015). A global boom in hydropower dam construction. *Aquatic Sciences*, *77*(1), 161–170. https://doi.org/10.1007/s00027-014-0377-0.

Zhang, H., Chen, G., Hu, J., Chen, S.-H., Wiedinmyer, C., Kleeman, M., & Ying, Q. (2014). Evaluation of a seven-year air quality simulation using the Weather Research and Forecasting (WRF)/Community Multiscale Air Quality (CMAQ) models in the eastern United States. The Science of the Total Environment, 473-474, 275–285. https://doi.org/10.1016/j.scitotenv.2013.11.121.

Zhou, Y., Zhou, L., Zhang, Y., Garcia de Souza, J., Podgorski, D. C., Spencer, R. G. M., Jeppesen, E., & Davidson, T. A. (2019). Autochthonous dissolved organic matter potentially fuels methane ebullition from experimental lakes. Water Research, 166, 115048. https://doi.org/10.1016/j.watres.2019.115048.

References cited in Supporting Information (and not included in above reference list)

Araújo, C. A. S., Sampaio, F. G., Alcântara, E., Curtarelli, M. P., Ogashawara, I., & Stech, J. L. (2017a). Effects of atmospheric cold fronts on stratification and water quality of a tropical reservoir: implications for aquaculture. Aquaculture Environment Interactions, 9, 385–403. https://doi.org/10.3354/aei00240.

Araújo, F. G., Morado, C. N., Parente, T. T. E., Paumgartten, F. J. R., & Gomes, I. D. (2017b). Biomarkers and bioindicators of the environmental condition using a fish species (Pimelodus maculatus Lacepède, 1803) in a tropical reservoir in Southeastern Brazil. Brazilian Journal of Biology, 78(2), 351–359. https://doi.org/10.1590/1519-6984.167209.

Beaulieu, J. J., Smolenski, R. L., Nietch, C. T., Townsend-Small, A., Elovitz, M. S., & Schubauer-Berigan, J. P. (2014). Denitrification alternates between a source and sink of nitrous oxide in the hypolimnion of a thermally stratified reservoir. *Limnology and Oceanograph*y, 59(2), 495–506. https://doi.org/10.4319/lo.2014.59.2.0495.

Beilfuss, R. (2010). Modelling trade-offs between hydropower generation and environmental flow scenarios: a case study of the Lower Zambezi River Basin, Mozambique. *International Journal of River Basin Management, 8*(3-4), 331–347. https://doi.org/10.1080/15715124.2010.533643.

Bergier, I., Evlyn M L, Ramos, F. M., Mazzi, E. A., & Maria F F. (2011). Carbon Dioxide and Methane Fluxes in the Littoral Zone of a Tropical Savanna Reservoir (Corumbá, Brazil). *Oecologia Australis, 15*(3), 666–681. https://doi.org/10.4257/oeco.2011.1503.17.

Bernardo, J. W. Y., Mannich, M., Hilgert, S., Fernandes, C. V. S., & Bleninger, T. (2017). A method for the assessment of long-term changes in carbon stock by construction of a hydropower reservoir. *Ambio, 46*(5), 566–577. https://doi.org/10.1007/s13280-016-0874-6.

Bevelhimer, M. S., Stewart, A. J., Fortner, A. M., Phillips, J. R., & Mosher, J. J. (2016). CO2 is Dominant Greenhouse Gas Emitted from Six Hydropower Reservoirs in Southeastern United States during Peak Summer Emissions. *Water, 8*(1), 15. https://doi.org/10.3390/w8010015.

Borges, P. A. F., Train, S., & Rodrigues, L. C. (2008). Spatial and temporal variation of phytoplankton in two subtropical Brazilian reservoirs. Hydrobiologia, 607(1), 63–74. https://doi.org/10.1007/s10750-008-9367-3.

Brothers, S. M., del Giorgio, P. A., Teodoru, C. R., & Prairie, Y. T. (2012). Landscape heterogeneity influences carbon dioxide production in a young boreal reservoir. *Canadian Journal of Fisheries and Aquatic Sciences,* 69(3), 447–456. https://doi.org/10.1139/f2011-174.

Bunting, L., Leavitt, P. R., Simpson, G. L., Wissel, B., Laird, K. R., Cumming, B. F., St. Amand, A., & Engstrom, D. R. (2016). Increased variability and sudden ecosystem state change in Lake Winnipeg, Canada, caused by 20thcentury agriculture: Lake Winnipeg Variability and State Change. Limnology and Oceanography, 61(6), 2090–2107. https://doi.org/10.1002/lno.10355.

Calijuri, M. C., & Dos Santos, A. C. A. (2001). Temporal variations in phytoplankton primary production in a tropical reservoir (Barra Bonita, SP--Brazil). Hydrobiologia, 445(1), 11–26. https://doi.org/10.1023/A:1017554829992.

Chanudet, V., Gaillard, J., Lambelain, J., Demarty, M., Descloux, S., Félix-Faure, J., Poirel, A., & Dambrine, E. (2020). Emission of greenhouse gases from French temperate hydropower reservoirs. *Aquatic Sciences, 82*(3). https://doi.org/10.1007/s00027-020-00721-3.

Cunha, D. G. F., Benassi, S. F., de Falco, P. B., & Calijuri, M. do C. (2016). Trophic State Evolution and Nutrient Trapping Capacity in a Transboundary Subtropical Reservoir: A 25-Year Study. *Environmental Management, 57*(3), 649–659. https://doi.org/10.1007/s00267-015-0633-7.

Deemer, B. R., Harrison, J. A., & Whitling, E. W. (2011). Microbial dinitrogen and nitrous oxide production in a small eutrophic reservoir: An in situ approach to quantifying hypolimnetic

process rates. *Limnology and Oceanograph, 56*(4), 1189–1199. https://doi.org/10.4319/lo.2011.56.4.1189.

De Lima, I. B. T., de Moraes Novo, E. M. L., Ballester, M. V. R., & Ometto, J. P. (1998). Methane production, transport and emission in Amazon hydroelectric plants. IGARSS '98. *Sensing and Managing the Environment. 1998 IEEE International Geoscience and Remote Sensing. Symposium Proceedings.* (Cat. No.98CH36174), 5, 2529–2531 vol.5. https://doi.org/10.1109/IGARSS.1998.702268.

DelSontro, T., McGinnis, D. F., Sobek, S., Ostrovsky, I., & Wehrli, B. (2010). Extreme Methane Emissions from a Swiss Hydropower Reservoir: Contribution from Bubbling Sediments. *Environmental Science & Technology, 44*(7), 2419–2425. https://doi.org/10.1021/es9031369.

Demarty, M., Bastien, J., & Tremblay, A. (2011). Annual follow-up of gross diffusive carbon dioxide and methane emissions from a boreal reservoir and two nearby lakes in Québec, Canada. *Biogeosciences, 8*(1), 41–53. https://doi.org/10.5194/bg-8-41-2011.

Demarty, M., Bastien, J., Tremblay, A., Hesslein, R. H., & Gill, R. (2009). Greenhouse Gas Emissions from Boreal Reservoirs in Manitoba and Québec, Canada, Measured with Automated Systems. *Environmental Science & Technology, 43*(23), 8908–8915. https://doi.org/10.1021/es8035658.

de Mello, N. A. S. T., Brighenti, L. S., Barbosa, F. A. R., Staehr, P. A., & Bezerra Neto, J. F. (2018). Spatial variability of methane (CH4) ebullition in a tropical hypereutrophic reservoir: silted areas as a bubble hot spot. *Lake and Reservoir Management, 34*(2), 105–114. https://doi.org/10.1080/10402381.2017.1390018.

Descloux, S., Chanudet, V., Serça, D., & Guérin, F. (2017). Methane and nitrous oxide annual emissions from an old eutrophic temperate reservoir. *The Science of the Total Environment, 598*, 959–972. https://doi.org/10.1016/j.scitotenv.2017.04.066.

Deshmukh, C., Serça, D., Delon, C., Tardif, R., Demarty, M., Jarnot, C., Meyerfeld, Y., Chanudet, V., Guédant, P., Rode, W., Descloux, S., & Guérin, F. (2014). Physical controls on CH4 emissions from a newly flooded subtropical freshwater hydroelectric reservoir: Nam Theun 2. Biogeosciences, 11(15), 4251–4269. https://doi.org/10.5194/bg-11-4251-2014.

De Vicente, I., Rueda, F., Cruz-Pizarro, L., & Morales-Baquero, R. (2008). Implications of seston settling on phosphorus dynamics in three reservoirs of contrasting trophic state.

Fundamental and Applied Limnology, 170(4), 263–272. https://doi.org/10.1127/1863-9135/2008/0170-0263.

Diem, T., Koch, S., Schwarzenbach, S., Wehrli, B., & Schubert, C. J. (2012). Greenhouse gas emissions (CO2, CH4, and N2O) from several perialpine and alpine hydropower reservoirs by diffusion and loss in turbines. *Aquatic Sciences, 74*(3), 619–635. https://doi.org/10.1007/s00027-012-0256-5.

Domingues, C. D., da Silva, L. H. S., Rangel, L. M., de Magalhães, L., de Melo Rocha, A., Lobão, L. M., Paiva, R., Roland, F., & Sarmento, H. (2017). Microbial Food-Web Drivers in Tropical Reservoirs. *Microbial Ecology, 73*(3), 505–520. https://doi.org/10.1007/s00248-016-0899-1.

dos Santos, M. A., Rosa, L. P., Sikar, B., Sikar, E., & dos Santos, E. O. (2006). Gross greenhouse gas fluxes from hydro-power reservoir compared to thermo-power plants. *Energy Policy, 34*(4), 481–488. https://doi.org/10.1016/j.enpol.2004.06.015.

Duchemin, E., Lucotte, M., Canuel, R., & Chamberland, A. (1995). Production of the greenhouse gases CH4 and CO2 by hydroelectric reservoirs of the boreal region. *Global Biogeochemical Cycles, 9*(4), 529–540. https://doi.org/10.1029/95GB02202.

Duchemin, E., Lucotte, M., Canuel, R., Queiroz, A. G., Almeida, D. C., Pereira, H. C., & Dezincourt, J. (2000). Comparison of greenhouse gas emissions from an old tropical reservoir with those from other reservoirs worldwide. *Verh. Internat. Verein. Limnol., 27*, 1391–1395. https://doi.org/10.1080/03680770.1998.11901464.

Dumestre, J. F., Casamayor, E. O., Massana, R., & Pedrós-Alió, C. (2002). Changes in bacterial and archaeal assemblages in an equatorial river induced by the water eutrophication of Petit Saut dam reservoir (French Guiana). *Aquatic Microbial Ecology: International Journal, 26*, 209–221. https://doi.org/10.3354/ame026209.

Filatov, N., & Rukhovets, L. (2012). Ladoga Lake and Onego Lake (Lakes Ladozhskoye and Onezhskoye). Encyclopedia of Earth Sciences Series, 429–432. https://elibrary.ru/item.asp?id=35731935

Gikas, G. D., Tsihrintzis, V. A., Akratos, C. S., & Haralambidis, G. (2009). Water quality trends in Polyphytos reservoir, Aliakmon River, Greece. *Environmental Monitoring and Assessment, 149*(1-4), 163–181. https://doi.org/10.1007/s10661-008-0191-z.

Grönlund, E., & Viljanen, M. (2003). Comparison of automatic and conventional physical and chemical analyses in Lake Saimaa, Eastern Finland. Hydrobiologia, 506-509(1-3), 59–65. https://doi.org/10.1023/b:hydr.0000008559.29601.f0.

Gruca-Rokosz, R. (2020). Quantitative Fluxes of the Greenhouse Gases CH4 and CO2 from the Surfaces of Selected Polish Reservoirs. *Atmosphere, 11*(3), 286. https://doi.org/10.3390/atmos11030286.

Gruca-Rokosz, R., & Tomaszek, J. A. (2015). Methane and Carbon Dioxide in the Sediment of a Eutrophic Reservoir: Production Pathways and Diffusion Fluxes at the Sediment–Water Interface. *Water, Air, & Soil Pollution, 226*(16). https://doi.org/10.1007/s11270-014-2268-3.

Guérin, F., Abril, G., Richard, S., Burban, B., Reynouard, C., Seyler, P., & Delmas, R. (2006). Methane and carbon dioxide emissions from tropical reservoirs: Significance of downstream rivers. *Geophysical Research Letters, 33*(L21407). https://doi.org/10.1029/2006gl027929.

Gunkel, G., Lange, U., Walde, D., & Rosa, J. W. C. (2003). The environmental and operational impacts of Curuá-Una, a reservoir in the Amazon region of Pará, Brazil. *Lakes & Reservoirs: Research and Management, 8*, 201–216. https://doi.org/10.1111/j.1440-1770.2003.00227.x.

Hardenbicker, P., Rolinski, S., Weitere, M., & Fischer, H. (2014). Contrasting long-term trends and shifts in phytoplankton dynamics in two large rivers: Long-term phytoplankton dynamics. *International Review of Hydrobiology, 99*(4), 287–299. https://doi.org/10.1002/iroh.201301680

Harrison, J. A., Deemer, B. R., Birchfield, M. K., & O'Malley, M. T. (2017). Reservoir Water-Level Drawdowns Accelerate and Amplify Methane Emission. *Environmental Science & Technology, 51*(3), 1267–1277. https://doi.org/10.1021/acs.est.6b03185.

Heikal, M. (2010). Impact of water level fluctuation on water quality and trophic state of lake Nasser and its khors, Egypt. Egyptian Journal of Aquatic Biology and Fisheries, 14(1), 75–86. https://doi.org/10.21608/ejabf.2010.2054.

Hilgert, S., Fernandes, C. V. S., & Fuchs, S. (2019). Redistribution of methane emission hot spots under drawdown conditions. *The Science of the Total Environment, 646*, 958–971. https://doi.org/10.1016/j.scitotenv.2018.07.338.

Huttunen, J. T., Väisänen, T. S., Hellsten, S. K., Heikkinen, M., Nykänen, H., Jungner, H., Niskanen, A., Virtanen, et al. (2002). Fluxes of CH4, CO2, and N2O in hydroelectric

reservoirs Lokka and Porttipahta in the northern boreal zone in Finland. *Global Biogeochemical Cycles, 16*(1), 3–1. https://doi.org/10.1029/2000GB001316.

Imberger, J., & Patterson, J. C. (1989). Physical Limnology. In J. W. Hutchinson & T. Y. Wu (Eds.), Advances in Applied Mechanics (Vol. 27, pp. 303–475). Elsevier. https://doi.org/10.1016/S0065-2156(08)70199-6

Johnson, D. M. (1985). Atlas of Oregon lakes. Oregon State University Press.

Joyce, J., & Jewell, P. W. (2003). Physical Controls on Methane Ebullition from Reservoirs and Lakes. *Environmental & Engineering Geoscience, 9*(2), 167–178. https://doi.org/10.2113/9.2.167.

Junet, A. de, de Junet, A., Abril, G., Guérin, F., Billy, I., & de Wit, R. (2009). A multi-tracers analysis of sources and transfers of particulate organic matter in a tropical reservoir (Petit Saut, French Guiana). *River Research and Applications, 25*(3), 253–271. https://doi.org/10.1002/rra.1152.

Karikari, A. Y., Akpabey, F., & Abban, E. K. (2013). Assessment of water quality and primary productivity characteristics of Volta Lake in Ghana. Academia Journal of Environmental Sciences, 1(5), 88–103. http://dx.doi.org/10.15413/ajes.2012.0109.

Kasper, D., Forsberg, B. R., Amaral, J. H. F., Leitão, R. P., Py-Daniel, S. S., Bastos, W. R., & Malm, O. (2014). Reservoir stratification affects methylmercury levels in river water, plankton, and fish downstream from Balbina hydroelectric dam, Amazonas, Brazil. Environmental Science & Technology, 48(2), 1032–1040. https://doi.org/10.1021/es4042644

Kehrig, H. A., Palermo, E. F. A., Seixas, T. G., Santos, H. S. B., Malm, O., & Akagi, H. (2009). Methyl and total mercury found in two man-made Amazonian Reservoirs. *Journal of the Brazilian Chemical Society, 20*(6), 1142–1152. https://doi.org/10.1590/s0103-50532009000600021.

Keller, M., & Stallard, R. F. (1994). Methane emission by bubbling from Gatun Lake, Panama. *Journal of Geophysical Research, 99*(D4), 8307. https://doi.org/10.1029/92jd02170.

Kelly, C. A., Rudd, J. W. M., St. Louis, V. L., & Moore, T. (1994). Turning attention to reservoir surfaces, a neglected area in greenhouse studies. Eos, 75(29), 332. https://doi.org/10.1029/94eo00987

King, A. “Priest Rapids Dam On Columbia River Leaking In Several Sections”. Northwest Public Broadcasting. April 10, 2018. https://www.nwpb.org/2018/04/10/priest-rapids-dam-leaking-in-several-sections/. Retrieved 16 February 2021.

Kunz, M. J., Anselmetti, F. S., Wüest, A., Wehrli, B., Vollenweider, A., Thüring, S., & Senn, D. B. (2011). Sediment accumulation and carbon, nitrogen, and phosphorus deposition in the large tropical reservoir Lake Kariba (Zambia/Zimbabwe). Journal of Geophysical Research, 116(G3). https://doi.org/10.1029/2010jg001538

León-Palmero, E., Morales-Baquero, R., & Reche, I. (2020). Greenhouse gas fluxes from reservoirs determined by watershed lithology, morphometry, and anthropogenic pressure. *Environmental Research Letters: ERL, 15*(4), 044012. https://doi.org/10.1088/1748-9326/ab7467.

Lieberman, D. M. & Grabowski, S. J. (2007). Physical, Chemical, and Biological Characteristics of Cle Elum and Bumping Lakes in the Upper Yakima River Basin, Storage Dam Fish Passage Study, Yakima Project, Washington, Technical Series No. PN-YDFP-005, Bureau of Reclamation, Boise, Idaho,March 2007.

Lima, I. B. T., Victoria, R. L., Novo, E. M. L. M., Feigl, B. J., Ballester, M. V. R., & Ometto, J. P. (2002). Methane, carbon dioxide and nitrous oxide emissions from two Amazonian Reservoirs during high water table. *SIL Proceedings, 1922-2010, 28*(1), 438–442. https://doi.org/10.1080/03680770.2001.11902620.

Lima, I. B. T. (2005). Biogeochemical distinction of methane releases from two Amazon hydroreservoirs. *Chemosphere, 59*(11), 1697–1702. https://doi.org/10.1016/j.chemosphere.2004.12.011.

“Lower Monumental Lock and Dam”. US Army Corps of Engineers, Walla Walla District Website. https://www.nww.usace.army.mil/Locations/District-Locks-and-Dams/Lower-Monumental-Lock-and-Dam/. Retrieved 16 February 2021.

Marcelino, A. A., Santos, M. A., Xavier, V. L., Bezerra, C. S., Silva, C. R. O., Amorim, M. A., Rodrigues, R. P., & Rogerio, J. P. (2015). Diffusive emission of methane and carbon dioxide from two hydropower reservoirs in Brazil. *Brazilian Journal of Biology, 75*(2), 331–338. https://doi.org/10.1590/1519-6984.12313.

Matsumura-Tundisi, T., Tundisi, J. G., Tundisi, M. E. J., & Cimbleris, A. (2006). Carbon content and composition of zooplankton fractions in two reservoirs of Central Brazil: Serra da Mesa

and Manso. *Verh. Internat. Verein. Limnol.*, *29*, 2237–2244. https://doi.org/10.1080/03680770.2006.11903089.

McClure, R. P., Lofton, M. E., Chen, S., Krueger, K. M., Little, J. C., & Carey, C. C. (2020). The magnitude and drivers of methane ebullition and diffusion vary on a longitudinal gradient in a small freshwater reservoir. *Journal of Geophysical Research: Biogeosciences, 125*(3). https://doi.org/10.1029/2019jg005205.

Miller, B. L., Arntzen, E. V., Goldman, A. E., & Richmond, M. C. (2017). Methane Ebullition in Temperate Hydropower Reservoirs and Implications for US Policy on Greenhouse Gas Emissions. *Environmental Management, 60*(4), 615–629. https://doi.org/10.1007/s00267-017-0909-1.

Mineeva, N. M., Semadeny, I. V., & Makarova, O. S. (2020). Chlorophyll content and the modern trophic state of the Volga river reservoirs (2017–2018). Inland Water Biology, 13(2), 327–330. https://doi.org/10.1134/s199508292002008x

Minns, C. K., & Shuter, B. J. (2013). A semi-mechanistic seasonal temperature-profile model (STM) for the period of stratification in dimictic lakes. Canadian Journal of Fisheries and Aquatic Sciences. Journal Canadien Des Sciences Halieutiques et Aquatiques, 70(2), 169–181. https://doi.org/10.1139/cjfas-2012-0253.

Montgomery, S., Lucotte, M., Pichet, P., & Mucci, A. (1995). Total dissolved mercury in the water column of several natural and artificial aquatic systems of Northern Quebec (Canada). In Canadian Journal of Fisheries and Aquatic Sciences (Vol. 52, Issue 11, pp. 2483–2492). https://doi.org/10.1139/f95-839.

Mosher, J. J., Fortner, A. M., Phillips, J. R., Bevelhimer, M. S., Stewart, A. J., & Troia, M. J. (2015). Spatial and Temporal Correlates of Greenhouse Gas Diffusion from a Hydropower Reservoir in the Southern United States. *Water, 7*(11), 5910–5927. https://doi.org/10.3390/w7115910.

Nanini-Costa, M. H., Quináglia, G. A., Petesse, M. L., & Esteves, K. E. (2017). Diet of an invading clupeid along an urban neotropical reservoir: responses to different environmental conditions. *Environmental Biology of Fishes, 100*(10), 1193–1212. https://doi.org/10.1007/s10641-017-0636-8.

Ometto, J. P., Cimbleris, A. C. P., dos Santos, M. A., Rosa, L. P., Abe, D., Tundisi, J. G., Stech, J. L., Barros, N., & Roland, F. (2013). Carbon emission as a function of energy generation in

hydroelectric reservoirs in Brazilian dry tropical biome. *Energy Policy, 58,* 109–116. https://doi.org/10.1016/j.enpol.2013.02.041.

Ogashawara, I., Alcântara, E., Curtarelli, M., Adami, M., Nascimento, R., Souza, A., Stech, J., & Kampel, M. (2014). Performance Analysis of MODIS 500-m Spatial Resolution Products for Estimating Chlorophyll-a Concentrations in Oligo- to Meso-Trophic Waters Case Study: Itumbiara Reservoir, Brazil. Remote Sensing, 6(2), 1634–1653. https://doi.org/10.3390/rs6021634.

Pacheco, F. S., Soares, M. C. S., Assireu, A. T., Curtarelli, M. P., Roland, F., Abril, G., Stech, J. L., Alvalá, P. C., & Ometto, J. P. (2015). The effects of river inflow and retention time on the spatial heterogeneity of chlorophyll and water-air CO 2 fluxes in a tropical hydropower reservoir. *Biogeosciences, 12,* 147-162. https://doi.org/10.5194/bg-12-147-2015.

PacifiCorp (2012). PacifiCorp Klamath Hydroelectric Project Interim Operations Habitat Conservation
Plan for Coho Salmon. Prepared by PacifiCorp Energy, Inc, Portland, OR. Submitted to the National Marine Fisheries Service, Arcata Area Office, Arcata, CA. February 16, 2012.

Poletaeva, V. I., Pastukhov, M. V., Zagorulko, N. A., & Belogolova, G. A. (2018). Changes in water hydrochemistry in bays of the bratsk reservoir caused by forest harvesting operations. Water Resources, 45(3), 369–378. https://doi.org/10.1134/s0097807818030119.

Rawson, D. S. (1960). A limnological comparison of twelve large lakes in Northern Saskatchewan. *Limnology & Oceanography.* 195 – 212. https://doi.org/10.4319/lo.1960.5.2.0195.

"Register of Large Dams in Australia". Dams information. Australian National Committee on Large Dams. 2010. Retrieved 16 February 2021.

Rodriguez, M., & Casper, P. (2018). Greenhouse gas emissions from a semi-arid tropical reservoir in northeastern Brazil. *Regional Environmental Change, 18*(7), 1901–1912. https://doi.org/10.1007/s10113-018-1289-7.

Rogério, J. P., Santos, M. A., & Santos, E. O. (2013). Influence of environmental variables on diffusive greenhouse gas fluxes at hydroelectric reservoirs in Brazil. Brazilian Journal of Biology = Revista Brasleira de Biologia, 73(4), 753–764. .

Roland, F., Vidal, L. O., Pacheco, F. S., Barros, N. O., Assireu, A., Ometto, J. P. H. B., Cimbleris, A. C. P., & Cole, J. J. (2010). Variability of carbon dioxide flux from tropical (Cerrado)

hydroelectric reservoirs. *Aquatic Sciences, 72*(3), 283–293. https://doi.org/10.1007/s00027-010-0140-0.

Rosa, L. P., Dos Santos, M. A., Matvienko, B., Sikar, E., Lourenço, R. S. M., & Menezes, C. F. (2003). Biogenic gas production from major Amazon reservoirs, Brazil. *Hydrological Processes, 17*(7), 1443–1450. https://doi.org/10.1002/hyp.1295.

Rosa, L. P., dos Santos, M. A., Matvienko, B., dos Santos, E. O., & Sikar, E. (2004). Greenhouse gas emissions from hydroelectric reservoirs in tropical regions. *Climatic Change, 66*, 9–21. https://doi.org/10.1023/b:clim.0000043158.52222.ee

Samiotis, G., Pekridis, G., Kaklidis, N., Trikoilidou, E., Taousanidis, N., & Amanatidou, E. (2018). Greenhouse gas emissions from two hydroelectric reservoirs in Mediterranean region. *Environmental Monitoring and Assessment, 190*(6), 363. https://doi.org/10.1007/s10661-018-6721-4.

Silva, L. C. da, Leone, I. C., Santos-Wisniewski, M. J. dos, Peret, A. C., & Rocha, O. (2012). Invasion of the dinoflagellate Ceratium furcoides (Levander) Langhans 1925 at tropical reservoir and its relation to environmental variables. *Biota Neotropica, 12*(2), 93–100. https://doi.org/10.1590/S1676-06032012000200010.

St. Louis, V. L., Kelly, C. A., Duchemin, É., Rudd, J. W. M., & Rosenberg, D. M. (2000). Reservoir Surfaces as Sources of Greenhouse Gases to the Atmosphere: A Global Estimate: Reservoirs are sources of greenhouse gases to the atmosphere, and their surface areas have increased to the point where they should be included in global inventories of anthropogenic emissions of greenhouse gases. *Bioscience, 50*(9), 766–775. https://doi.org/10.1641/0006-3568(2000)050[0766:RSASOG]2.0.CO;2

Tadonléké, R. D., Marty, J., & Planas, D. (2012). Assessing factors underlying variation of CO2 emissions in boreal lakes vs. reservoirs. *FEMS Microbiology Ecology, 79*(2), 282–297. https://doi.org/10.1111/j.1574-6941.2011.01218.x.

Teodoru, C. R., Bastien, J., Bonneville, M.-C., del Giorgio, P. A., Demarty, M., Garneau, M., Hélie, J.-F., Pelletier, L., Prairie, Y. T., Roulet, N. T., & Others. (2012). The net carbon footprint of a newly created boreal hydroelectric reservoir. *Global Biogeochemical Cycles, 26*(2). https://agupubs.onlinelibrary.wiley.com/doi/abs/10.1029/2011GB004187.

Teodoru, C. R., Nyoni, F. C., Borges, A. V., Darchambeau, F., Nyambe, I., & Bouillon, S. (2015). Dynamics of greenhouse gases (CO2, CH4, N2O) along the Zambezi River and major

tributaries, and their importance in the riverine carbon budget. *Biogeosciences, 12*(8), 2431–2453. https://doi.org/10.5194/bg-12-2431-2015.

Therrien, J., Tremblay, A. & Jacques, R. B. (2005) in *Greenhouse Gas Emissions- Fluxes and Processes: Hydroelectric Reservoirs and Natural Environments*, eds. Tremblay, A., Varfalvy, L., Roehm, C. & Garneau, M. Springer.

Thornton, J. A. (1987). A review of some unique aspects of the limnology of shallow Southern African man-made lakes. *GeoJournal, 14*(3). https://doi.org/10.1007/bf00208207.

Tremblay, A., Therrien, J., Hamlin, B., Wichmann, E. & LeDrew, L. J. (2005) in *Greenhouse gas emissions-- fluxes and processes hydroelectric reservoirs and natural environments,* eds. Tremblay, A., Varfalvy, L., Roehm, C. & Garneau, M. pp 209–232. Springer.

Vörösmarty, C. J., Meybeck, M., Fekete, B., Sharma, K., Green, P., & Syvitski, J. P. M. (2003). Anthropogenic sediment retention: major global impact from registered river impoundments. Global and Planetary Change, 39(1), 169–190. https://doi.org/10.1016/S0921-8181(03)00023-7.

Weissenberger, S., Lucotte, M., & Canuel, R. (2012). The carbon cycle of Quebec boreal reservoirs investigated by elemental compositions and isotopic values. Biogeochemistry 111(1-3), 555–568. https://doi.org/10.1007/s10533-011-9687-7.

Wilander, A., & Persson, G. (2001). Recovery from eutrophication: experiences of reduced phosphorus input to the four largest lakes of Sweden. Ambio, 30(8), 475–485. https://doi.org/10.1579/0044-7447-30.8.475

Wilkinson, J., Bodmer, P., & Lorke, A. (2019). Methane dynamics and thermal response in impoundments of the Rhine River, Germany. *The Science of the Total Environment, 659,* 1045–1057. https://doi.org/10.1016/j.scitotenv.2018.12.424.